

Stephen F. Austin State University

**SFA ScholarWorks**

---

Electronic Theses and Dissertations

---

12-2016

## **Geotechnical Properties Of the Travis Peak (Hosston) Formation in East Texas: A Compressive and Tensile Strength Analysis using Regression Analysis.**

Pawan Kakarla

Stephen F Austin State University, pawank.1224@gmail.com

Follow this and additional works at: <https://scholarworks.sfasu.edu/etds>



Part of the [Geology Commons](#), and the [Geotechnical Engineering Commons](#)

[Tell us](#) how this article helped you.

---

### **Repository Citation**

Kakarla, Pawan, "Geotechnical Properties Of the Travis Peak (Hosston) Formation in East Texas: A Compressive and Tensile Strength Analysis using Regression Analysis." (2016). *Electronic Theses and Dissertations*. 62.

<https://scholarworks.sfasu.edu/etds/62>

This Thesis is brought to you for free and open access by SFA ScholarWorks. It has been accepted for inclusion in Electronic Theses and Dissertations by an authorized administrator of SFA ScholarWorks. For more information, please contact [cdsscholarworks@sfasu.edu](mailto:cdsscholarworks@sfasu.edu).

---

## Geotechnical Properties Of the Travis Peak (Hosston) Formation in East Texas: A Compressive and Tensile Strength Analysis using Regression Analysis.

### Creative Commons License



This work is licensed under a [Creative Commons Attribution-Noncommercial-No Derivative Works 4.0 License](https://creativecommons.org/licenses/by-nc-nd/4.0/).

GEOTECHNICAL PROPERTIES OF THE TRAVIS PEAK (HOSSTON)  
FORMATION IN EAST TEXAS: A COMPRESSIVE AND TENSILE  
STRENGTH ANALYSIS USING REGRESSION ANALYSIS.

By

PAWAN KAKARLA, Master of  
Technology

Presented to the Faculty of the Graduate School of  
Stephen F. Austin State University

In Partial Fulfillment  
Of the Requirements

For the Degree of  
Master of Science

STEPHEN F. AUSTIN STATE UNIVERSITY

December, 2016

GEOTECHNICAL PROPERTIES OF THE TRAVIS PEAK (HOSSTON)  
FORMATION IN EAST TEXAS: A COMPRESSIVE AND TENSILE  
STRENGTH ANALYSIS USING REGRESSION ANALYSIS.

PAWAN KAKARLA, Master of Technology.

APPROVED:

---

Dr. Wesley Brown, Thesis Director

---

Dr. Chris Barker, Committee Member

---

Dr. R. LaRell Nielson, Committee Member

---

Dr. Kent Riggs, Committee Member

---

Richard Berry, D.M.A

Dean of the Graduate School

## ABSTRACT

The estimation of rock mass strength is a key parameter in geotechnical engineering which is used in the design of geotechnical structures like tunnels, dams and slopes. Geotechnical engineering is the branch of civil engineering which works on the principles of soil and rock mechanics to evaluate subsurface conditions, stability of slopes, foundations of structures and construction of earthworks. The main focus of this study was to calculate the strength of Lower Cretaceous Travis Peak Formation rocks of East Texas and to check the accuracy by comparing it with Regression analysis. The parameters which were used were the Uniaxial Compression Test (UCS) and tensile strength.

Core samples were collected at Stephen F. Austin State University Core Lab Repository. Strength tests were conducted at the lab facilities of University of Houston.

Parameters such as load for UCS and tensile strength were experimentally determined using procedures outlined by the International Society of Rock Mechanics (ISRM, Rock characterization testing and monitoring, 1981). In this study, a linear regression analysis was also performed to predict and compare the strength values of the core rock samples from the Travis Peak Formation.

Based on previous studies, it was shown that regression analysis is accurate in providing the strength of rocks. The results obtained from the tests are useful in predicting the strength of rocks from the Travis Peak Formation.

Uniaxial compression and tensile strength tests were performed for 12 samples at the Department of Civil Engineering's Laboratory at the University of Houston. Before the tests, the samples were cut before into the size of 7.2 to 3.6 in ratio of length to diameter to maintain a 2:1 ratio.

The average value of UCS for the 12 samples was 27.43 MPa. Similarly, the average value for tensile strength for 12 samples was 4.05 MPa. Based on the values which were calculated, these samples were classified as medium strength rocks which belongs to Class D.

Linear Regression analysis was performed using MATLAB software for predicting the strength of core rock samples. The equation for linear regression was in the form of  $Y_1 = 0.1005 \times X_1 + (1.293)$ , where y is the tensile strength and x is UCS. The root mean square generated for regression analysis was 0.6378.

## ACKNOWLEDGMENTS

I would like to thank Dr. Cumaraswamy Vipulanandan, Professor at the Department of Civil and Environmental Engineering, University of Houston for allowing me to use their laboratory so that I was able to finish my testing on uniaxial compressive strength and tensile strength. I would especially thank Mr. Anudeep Reddy, graduate student at the Department of Civil and Environmental Engineering, University of Houston for assisting me in completion of this work. His assistance in preparing the samples and using the instrument for testing were invaluable.

I would like to thank Dr. Wesley Brown, my graduate advisor, for allowing me the freedom to complete this work on my own schedule and for being incredibly patient and understanding during this process. I would like to thank each member of my final thesis committee and the support of my family and friends.

## TABLE OF CONTENTS

ABSTRACT .....	i
ACKNOWLEDGMENTS .....	iii
LIST OF TABLES .....	ix
LIST OF EQUATIONS .....	x
OBJECTIVE .....	1
INTRODUCTION .....	2
REGIONAL SETTING .....	4
STRATIGRAPHIC SETTING .....	14
UNIAXIAL COMPRESSIVE TEST .....	24
Point load test to determine compressive strength .....	28
Point load strength index ( $I_s$ ) .....	28
Correlation between point load strength and uniaxial compressive strength .....	29
Compressive strength from Schmidt Hammer test .....	30
TENSILE STRENGTH .....	36
Splitting Tensile Test .....	36
Flexure Test .....	40
Regression Analysis .....	46



Independent variables and Dependent variables .....	49
RESULTS .....	52
Uniaxial Compressive Strength.....	52
Tensile Strength.....	57
Regression Analysis .....	62
Uniaxial Compressive Strength vs Tensile Strength .....	62
Box Plots .....	64
DISCUSSION .....	67
CONCLUSIONS.....	68
FUTURE WORK.....	70
REFERENCES .....	71
APPENDIX A – CORE SAMPLES DATABASE.....	78
APPENDIX B – HAND SAMPLE DESCRIPTIONS.....	81
VITA.....	90

## LIST OF FIGURES

Figure 1 – Gulf of Mexico’s geologic framework showing crustal types ( T. C. - Transitional continental crust; O. C. – Oceanic Crust) and depth to the top of the basement (Galloway, 2009). .....	6
Figure 2 - Map showing the tectonic setting of the East Texas Basin, adapted from (Martin, 1978).....	7
Figure 3 – Map showing the location of the East Texas basin, Houston embayment, Brazos basin and the other structural features of east Texas (Davidoff, 1991). .....	8
Figure 4 – Structural cross sections across the East Texas Basin (Wood & Guevara, 1981). .....	10
Figure 5 – Map area showing East Texas counties and the location of wells that were used in this study. The samples are taken from the highlighted counties. ....	11
Figure 6 – Stratigraphic column of the East Texas basin; highlighted portion showing the Travis Peak Formation (modified from (Arkansas Geological Survey, 2016))......	15
Figure 7 - Structure, top of the Cotton Valley Group Sandstone (base of Travis Peak Formation), showing the location of this study (modified from (Finley, 1984))......	16
Figure 8 – Image showing the arrangement of Unconfined Compression test which can hold up to a core sample of NX size and in the center is the sample taken from a core which has a length to diameter ratio of 2 (Geocomp Corp, 2015).....	27

Figure 9 – L type Schmidt Hammer, where A is the needle which is placed at the surface of the rock and B is the scale of the hammer which is used to measure the strength in MPa (Proceq, 2016). ..... 31

Figure 10 – N type Schmidt Hammer, where A is the needle which is placed at the surface of the rock and B is scale of the hammer which is used to measure the strength in MPa (PCTE, 2016)..... 32

Figure 11 – Image showing the arrangement of Tensile strength, which can also hold up a core size of NX size, and a length to diameter ratio of 4 or 5 (Istone, n.d.) ..... 38

Figure 12 – Horizontal and Vertical stresses measured from Splitting tensile test (Building Research Institute, 2016). ..... 39

Figure 13 – Image showing a core rock sample which was tested for UCS and Tensile strength which was cut into dimensions of 3.6 in width and 7.2 in length. .... 44

Figure 14 – Equipment used for testing the compressive strength and tensile strength at University of Houston’s Civil Engineering Laboratory. The same equipment is used to test the UCS and Tensile strength and the samples are rested on the instrument depending upon the test and the load is applied. .... 45

Figure 15–Image showing the equation for the linear regression analysis and the trendline (University of Washington, 2016). ..... 48

Figure 16–The above figure shows three different types of linear regression equations. First image shows a positive trend of the linear equation which has

a positive slope. Second one shows a negative trend of the linear equation which has a negative slope. Third one is a non-linear equation (Laerd Statistics, 2016).....	48
Figure 17 – Top and bottom of the samples are flattened by adding Sulfur which is melted at 300° F. ....	54
Figure 18 – Failure from the maximum stress plane ( $\sigma_1$ ) results in the uniaxial compressive strength test. ....	55
Figure 19–A plot showing the frequency histogram for UCS with the maximum number of 6 samples lie in the range of 28.23 to 43.23 MPa and minimum number of 1 sample lying in the range of 43.23 to 58.23 MPa.....	58
Figure 20 - Failure from minimum stress plane ( $\sigma_3$ ) results in tensile strength.....	59
Figure 21–A plot showing the frequency histogram for Tensile strength, where the maximum number of 6 samples lying in the range of 3.59 to 5.49 MPa and a minimum of 2 samples lying in the range of 5.49 to 7.39 MPa.....	61
Figure 22 – A plot showing linear regression analysis between Uniaxial Compressive Strength and Tensile strength which has a R-square value of 0.6378. ....	63
Figure 23 – Box plot showing the difference in the values between UCS and Tensile strength. The y-axis is strength in MPa. ....	65

## LIST OF TABLES

Table 1 – Various strength classification of intact rock (Bieniawski, 1984).....	26
Table 3 – Various classifications of point load strength index ( $I_s$ ) after (Bieniawski, 1984). .....	28
Table 4 – Various classification of k after (Palmstrom, 2011), where D is diameter.....	29
Table 5 – Compressive Strength of rocks from field identification (ISRM, 1978) .....	34
Table 6 – Strength classification of intact and jointed rocks (Ramamurthy & Arora, 1993). .....	43
Table 7–Table showing the data generated from the laboratory equipment for UCS and Tensile strength. ....	66
Table 8 - Table showing details on the core samples that must be used for the testing. ..	78

## LIST OF EQUATIONS

(1) $\sigma_c = k \times I_s$ .....	29
(2) $f_{bt} = Pl \div bd^2$ .....	40
(3) $y = \beta x + \epsilon$ .....	49
(4) UCS (lb/in <sup>2</sup> ) = Load (P in lbf)/Area (inches <sup>2</sup> ).....	53
(5) $T = 2P\pi DL$ .....	57
(6) $Y_1 = 0.1005 \times X_1 + (1.293)$ .....	62

## OBJECTIVE

The objectives of this study are to calculate uniaxial compressive strength and tensile strength of rocks in core samples from the Travis Peak Formation in East Texas and then predict the values using Linear Regression Analysis. These objectives are accomplished by using following methods:

1. Measuring the load for uniaxial compressive strength and tensile strength tests.
2. Calculating the uniaxial compressive strength and tensile strength using the measured load.
3. Predicting the strength values for rock samples from the Travis Peak Formation using linear regression analysis.

## INTRODUCTION

The most widely used techniques to determine the strength of rock masses are the uniaxial compressive strength (UCS) and tensile strength tests (Çanakçı, Baykasoğlu, & Güllü, 2009). Uniaxial compressive strength is a compressive strength of the material to withstand loads which has a tendency to reduce the size. UCS is the test which can resist compression. Similarly, Tensile strength is the strength of a material which can withstand loads and has a tendency to elongate. Tensile strength can resist tension. There are two ways to approach this. Firstly, there is the direct approach which involves collecting and testing the specimens in the laboratory. Secondly, there is the indirect approach which is to make use of previously determined empirical equations from the literature (Baykasoğlu, Güllü, Çanakçı, & Özbakir, 2008). A standard procedure for this testing was followed based on (ASTM D 2938-95), (ASTM D 3967-95a) and (ISRM, Rock characterization testing and monitoring, 1981). The acronym ASTM stands for the American Society of the International Association for Testing and Materials. It develops and publishes standards for testing of various materials and products. ISRM stands for the International Society for Rock Mechanics. The major function of ISRM is to publish standards for all tests that are used in studies related to rock mechanics, civil engineering, mining and petroleum engineering. In this study, all the tests are conducted based on the standards set by the ISRM.

Experimental tests for measuring UCS and tensile strength are preferred for designs and modeling. However, indirect methods are quite frequently used because they are simpler, faster and economical, particularly under limited laboratory testing



conditions (Çanakçı, Baykasoğlu, & Güllü, 2009). Indirect methods include simple index test variables such as impact strength and point load index to estimate UCS (Fener, Kahraman, Bilgil, & Gunaydin, 2005). Empirical equations are also used to calculate tensile strength.

The main aim was to calculate the uniaxial compressive strength and tensile strength of the core rock samples from the laboratory methods. Based on the calculations, linear regression analysis was used to predicting the strength of the core rock samples. The input variables that were used are UCS load, tensile strength load and area. UCS and tensile strength are the parameters that were predicted, thus they are the output variables.

## REGIONAL SETTING

The Gulf of Mexico basin (Figure 1) is a site of deposition of great thicknesses of Mesozoic and Cenozoic sediments, which attain a maximum basinward thickness of roughly 50,000 feet (Walper et al., 1979). The Gulf of Mexico is a relatively small oceanic basin with an area of slightly more than 579,000 mi<sup>2</sup> (1.5 million km<sup>2</sup>) (Martin, 1984). The present form of the basin was influenced by a combination of rifting and intrabasin sedimentary-tectonic processes during and after the Mesozoic Era (Murray & Others, 1985). The Ouachita tectonic belt parallels the northern and western rim of the Gulf of Mexico basin and extends across central and northeast Texas (where it is buried), southeast Oklahoma, southern Arkansas, and northern Mississippi (Figure 3) (Foote, Massingill, & Wells, 1988).

The East Texas basin is one of three Mesozoic basins in East Texas (Figure 2). The other two basins are the Brazos basin and the Houston embayment. The Brazos basin is thought to have formed during the opening of the Gulf of Mexico, which trended as a northeast half-graben (Davidoff, 1991). “The axis of the basin is marked by an elongate grouping of six salt diapirs and thickening of the overlying Jurassic and Lower Cretaceous strata” (Davidoff, 1991). The tectonic setting of the East Texas Basin can be seen in (Figure 3). Northwest-verging folds and thrusts were generated by compression of marine deposits during the Ouachita orogeny and stratal shortening (Jackson M. P., 1982). After that event, the Gulf of Mexico opened and “Initial subsidence due to rifting and crustal attenuation combined with subsequent sediment loading has caused a

maximum subsidence of more than 23,000 ft (7,010 m) in the center of the basin”  
(Jackson & Seni, 1984).

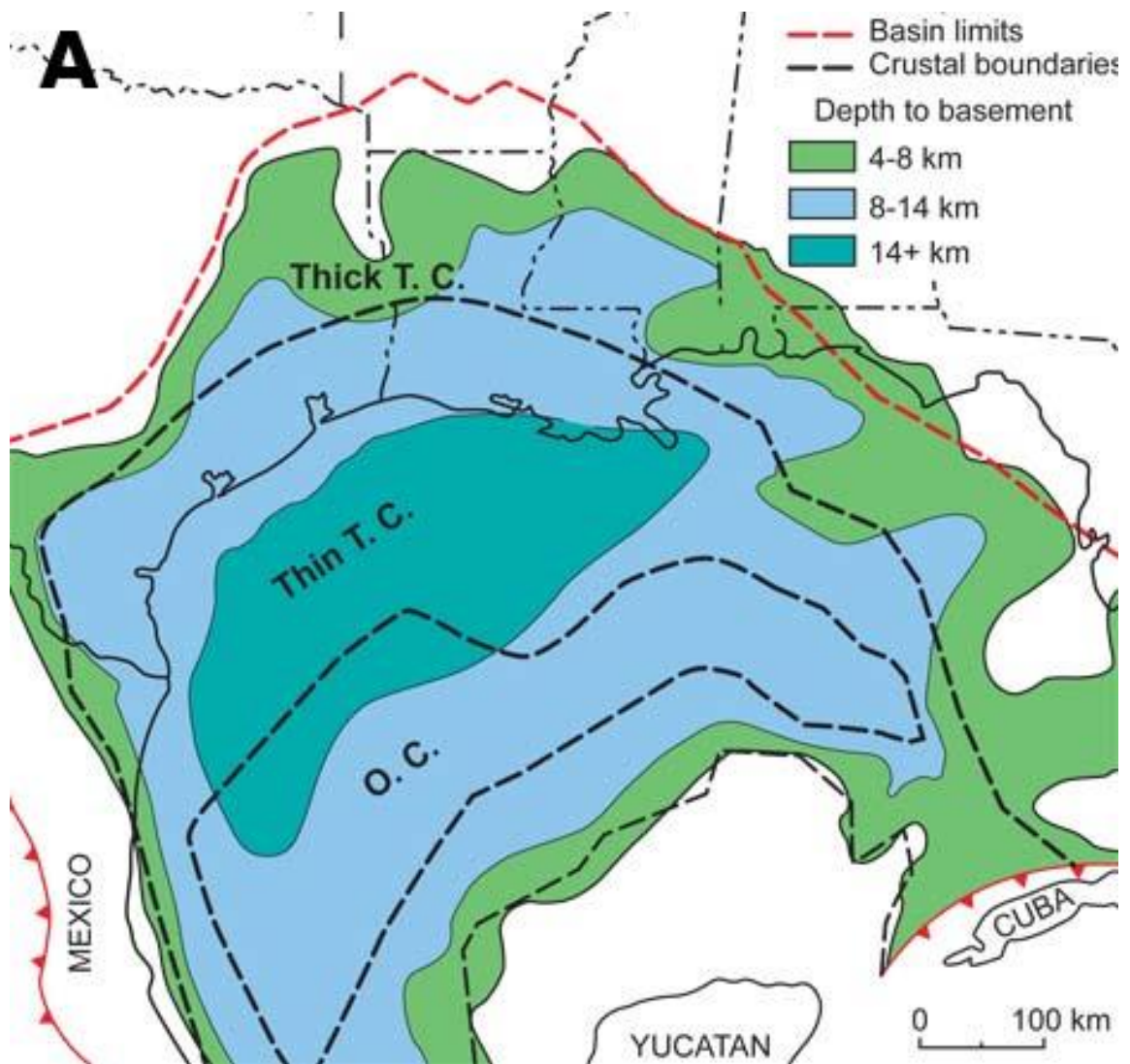


Figure 1–Gulf of Mexico’s geologic framework showing crustal types ( T. C. - Transitional continental crust; O. C. – Oceanic Crust) and depth to the top of the basement (Galloway, 2009).

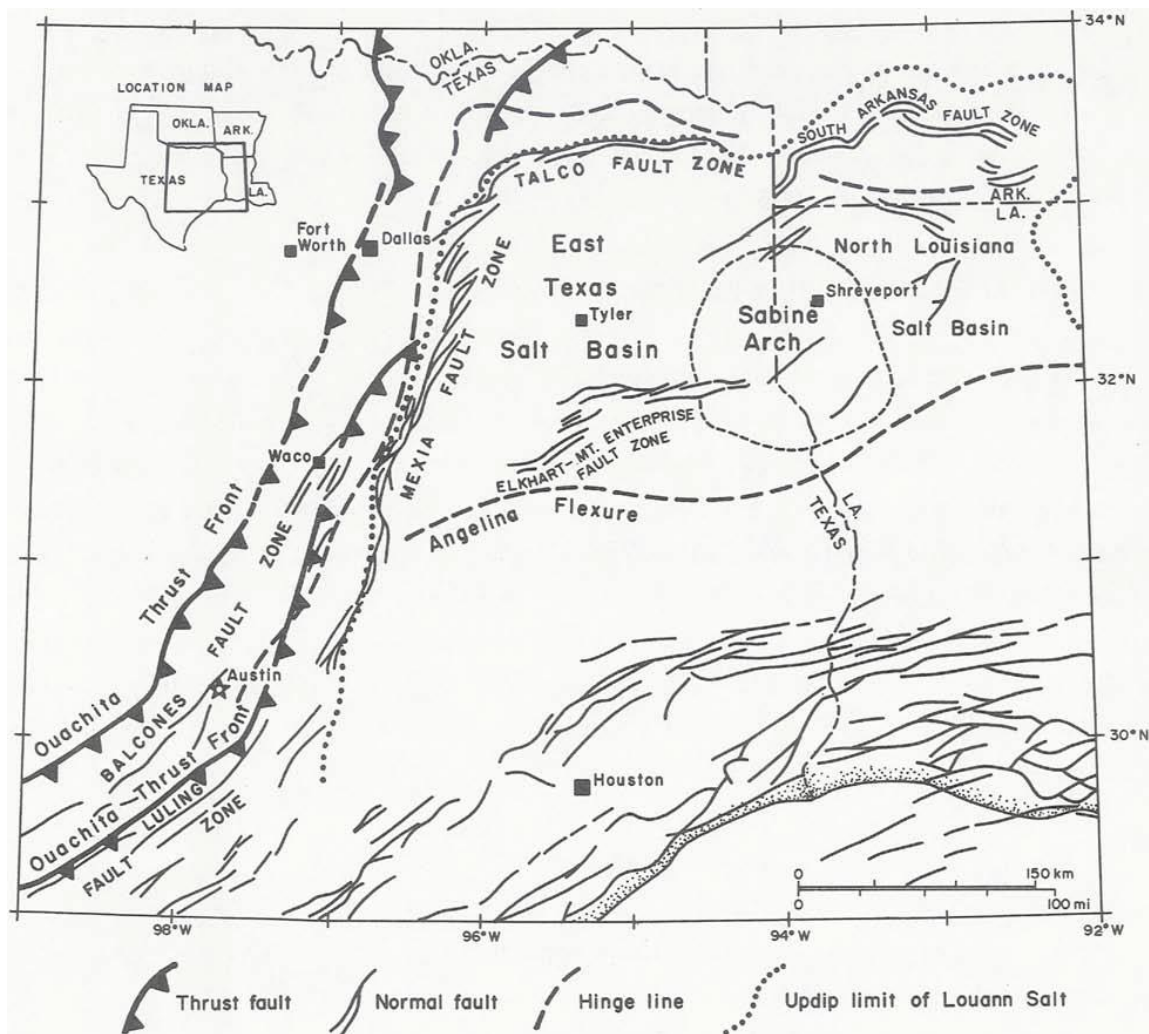


Figure 2—Map showing the tectonic setting of the East Texas Basin, adapted from (Martin, 1978)

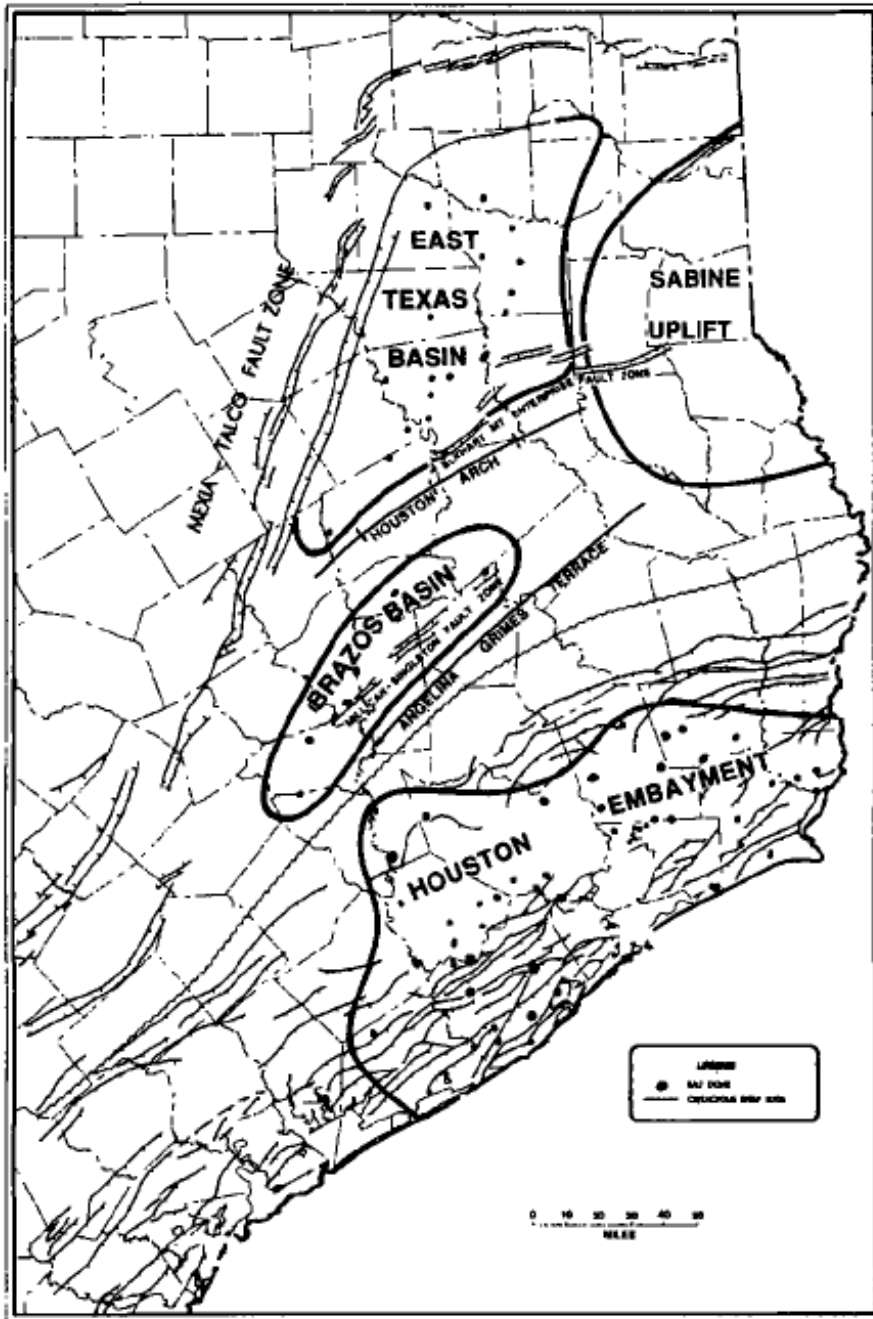


Figure 3—Map showing the location of the East Texas basin, Houston embayment, Brazos basin and the other structural features of east Texas (Davidoff, 1991).

As the Gulf of Mexico basin periodically filled with sea water, the evaporitic Louann Salt was deposited on an eroded post-rift, pre-breakup terrane which was due to the further subsidence of the marine incursions (Jackson M. P., 1982). “From (Figure 3) the updip limit of the Louann Salt is parallel to the Ouachita trends, because the Ouachita area during the Jurassic was still at some elevation as compared to subsiding East Texas Basin” (Jackson M. P., 1982). A monoclinial hinge line is present updip of the Louann Salt which is poorly defined. This hinge line is too weak to delineate the western and northern margins of the basin (Jackson M. P., 1982). Therefore, this part of the basin is defined by the Mexia-Talco Fault Zone. “Mexia-Talco Fault Zone is a peripheral graben system, which is active from the Jurassic to the Eocene that coincides with the updip limit of the Louann Salt (Jackson M. P., 1982).”

On the eastern margin of the basin is a structural dome, the Sabine Arch. The Angelina Flexure is a hinge line which defines the southern margin of the basin. It is generally a monocline at the ends and an anticlinal in the middle (Jackson M. P., 1982). The overall structure of the East Texas Basin consists of dips towards the basin in the east, west and north (Figure 4). “Major deformation within the basin is due to salt creep gravitationally (Jackson M. P., Fault tectonics of the East Texas Basin, 1982).”

Well sites for potential cores from the East Texas region that must have been used in this study are shown in Figure 5.

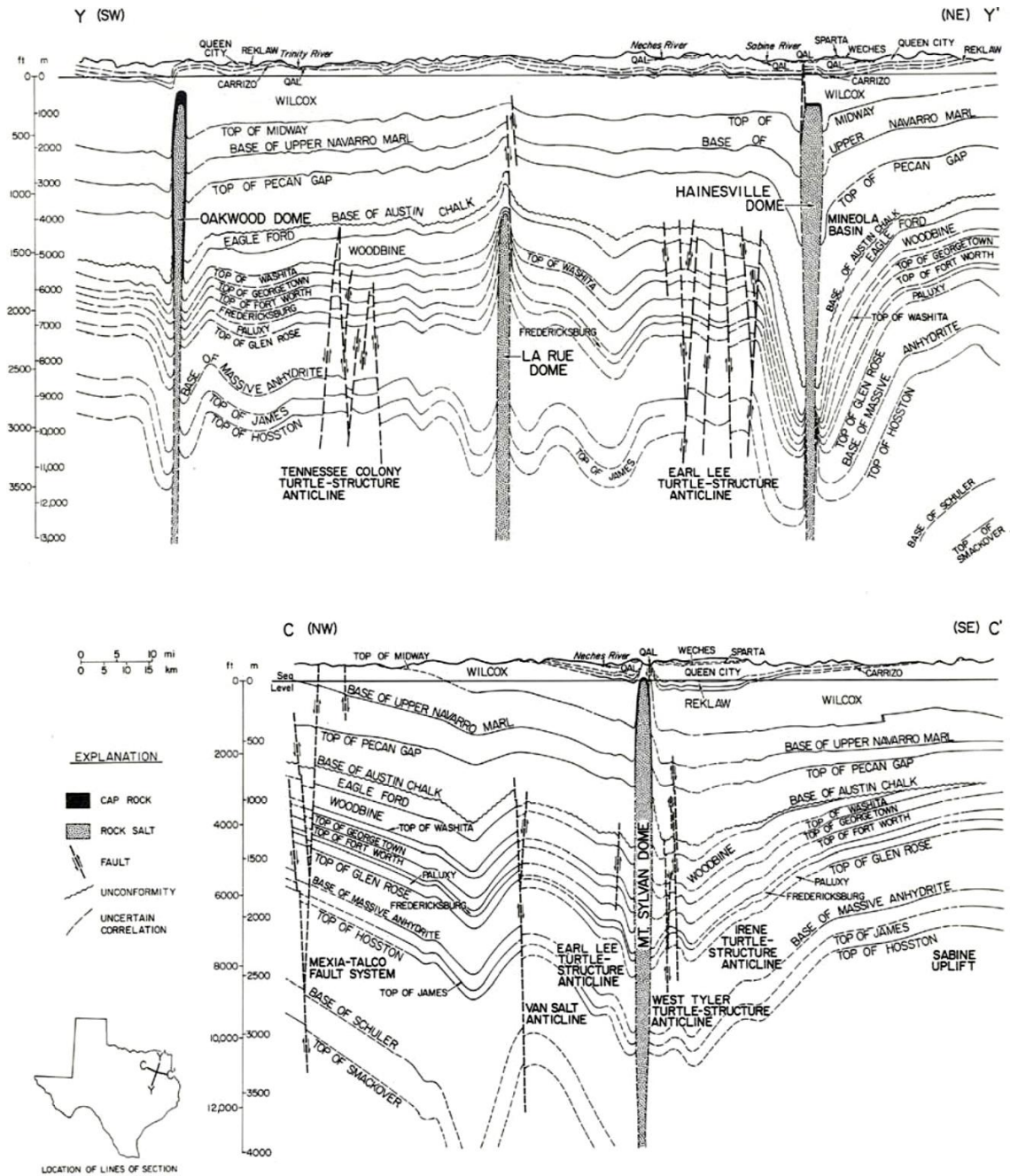


Figure 4—Structural cross sections across the East Texas Basin (Wood & Guevara, 1981).



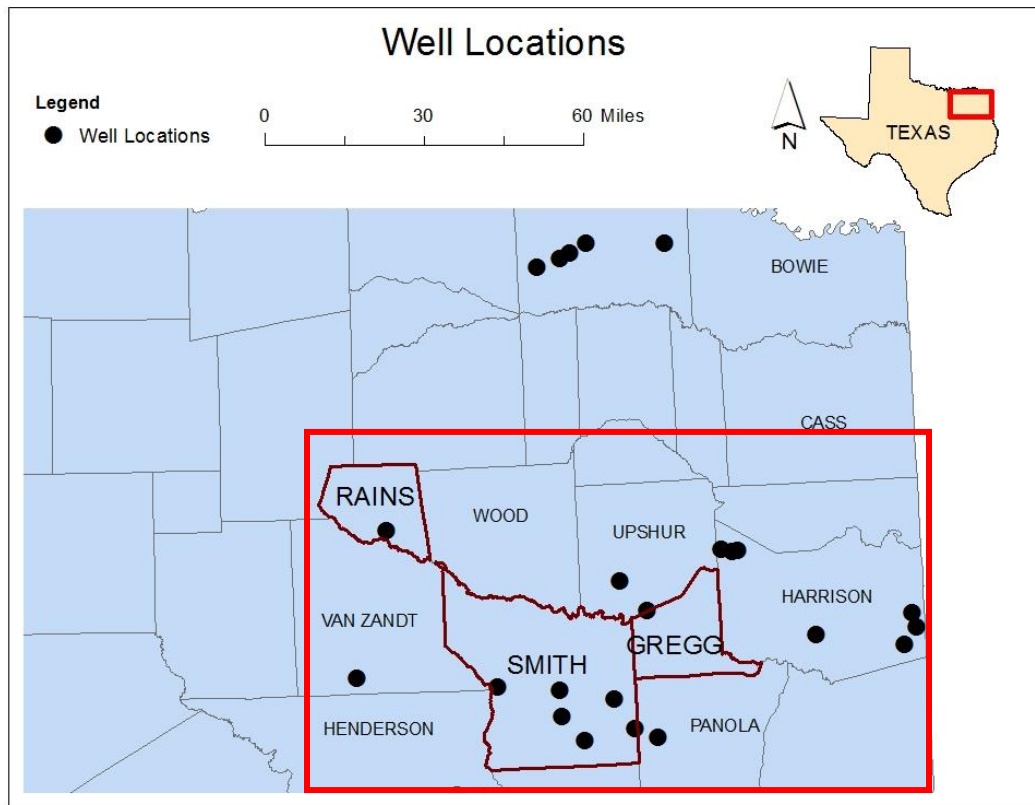


Figure 5–Map area showing East Texas counties and the location of wells that were used in this study. The samples are taken from the highlighted counties.

A complex system of rift basins or rhomb grabens were formed on the thinner continental crust in south Texas, east Texas, north Louisiana, central Mississippi-southwest Alabama and the Florida Panhandle at the early stage of continental separation during the Triassic Period. These rift basins and blocks developed into the Rio Grande embayment, East Texas basin, north Louisiana basin, Mississippi interior basin and the Apalachicola embayment respectively (Foote, Massingill, & Wells, 1988) (Figure 2). The Jurassic Louann salt developed in what at the time was a hypersaline restricted basin and the salt lies unconformably on Triassic rift sediments and Paleozoic basement rock.

Mexia-Talco Fault Zone: Consists of narrow grabens which are formed by strike-parallel normal faults. “The Great Bend is a zone of en-echelon normal faults which connect these two zones of parallel faults” (Jackson M. P., 1982). The location of the Mexia Fault Zone was mainly controlled by Triassic rift faults and by the updip limit of the Louann Salt, as the fault zone overlies the boundary fault of a half-graben containing Eagle Mills red beds (Jackson & Harris , 1981).

Central Basin-Faults: This is the salt-pillow province and the salt-diapir province of the East Texas Basin. Deep subsurface strata are rich in parallel normal faults. These faults form grabens more than 100 km long, parallel to the Mexia-Talco Fault Zone in deep Jurassic Strata. Over larger salt-related anticlines, there are faults in the center of the basin in Cretaceous horizons. On the crests of anticlinal structures such as salt pillows

and turtle structures, the orientation of these faults is parallel to the hinge lines of the anticlines and indicates the splitting of the structures by fold-related extension.

Elkhart Graben: The western end of the Elkhart-Mount Enterprise Fault Zone consists of the Elkhart Graben. This is made of parallel normal faults which are approximately 40 km long (Jackson M. P., 1982). “This graben forms the southern component of a fan of central-basin faults, which trend towards Oakwood Dome on the southwest margin of the basin (Jackson M. P., 1982)”. The Elkhart Graben’s origin is derived from the fault geometry which is also applied to the central-basin faults. Collins and others defined (1980) normal faults which are exposed in the Trinity River along the strike of the northern flank of the Elkhart Graben.

## STRATIGRAPHIC SETTING

In the northern Gulf coast, the Cretaceous System is made of 6000 to 9000 feet of fine to coarse terrigenous and marine clastics, carbonates, and interbedded evaporites and bioclastic materials (Warner, 1993). Upper Cretaceous units transgressed over older Mesozoic units because of a significant rise in sea level during the Cretaceous and also because there was an increase in the subsidence rates in the coastal margins at that time (Rainwater, *Stratigraphy and its role in future exploration of oil and gas in Gulf Coast*, 1960).

The Cretaceous system can be divided into Upper and Lower Cretaceous series (Figure 6) (Warner, 1993). The Lower Cretaceous can be further divided into the Hosston (Travis Peak), Sligo, Pine Island, James, Travis Peak, Ferry Lake, Mooringsport, Paluxy, Washita – Fredericksburg and Dantzler Formations. The Upper Cretaceous includes the Tuscaloosa, Eutaw (Austin), and Selma Formations (Dockery, 1981).

A transgression began during the Lower Cretaceous (Hosston) and concluded in a maximum highstand during the Late Selma which is the closing of the Upper Cretaceous (Warner, 1993). Sea level reached a maximum highstand during the late Cretaceous and thereafter the amount of terrigenous materials diminished and subsidence slowed in the northern Gulf Coast (Warner, 1993).

ERA	SYSTEM	SERIES	GROUP	FORMATION	
CENOZOIC	TERTIARY	Eocene	Clairborne	Cockfield	
				Cook Mountain	
				Sparta	
				Cane River	
			Wilcox	Wilcox	
		Paleocene	Midway	Midway	
	MESOZOIC	UPPER CRETACEOUS	GULFIAN	Navarro	Arkadelphia
					Nacatach
					Saratoga
				Taylor	Marlbrook
				Annona	
				Ozan	
				Brownstown	
Austin				Tokio	
Eagle Ford				Eagle Ford	
Tuscaloosa				Tuscaloosa (Woodbine)	
LOWER CRETACEOUS		COMANCHEAN		Washita-Fredericksburg	
				Paluxy	
			Trinity	Lower Glen Rose	Mooringsport
				Upper Glen Rose	Ferry Lake
					Rodessa
				James	
				Pine Island	
		COAHUILIAN	Nuevo Leon	Sligo	
				Travis Peak (Hosston)	
		JURASSIC	UPPER	Cotton Valley	Schuler
	Bossier				
Louark			Haynesville (Buckner Member)		
			Smackover		
			Norphlet		
MIDDLE		Louann Salt			
		Werner			
TRIASSIC	UPPER		Eagle Mills		

Figure 6–Stratigraphic column of the East Texas basin; highlighted portion showing the Travis Peak Formation (modified from (Arkansas Geological Survey, 2016)).

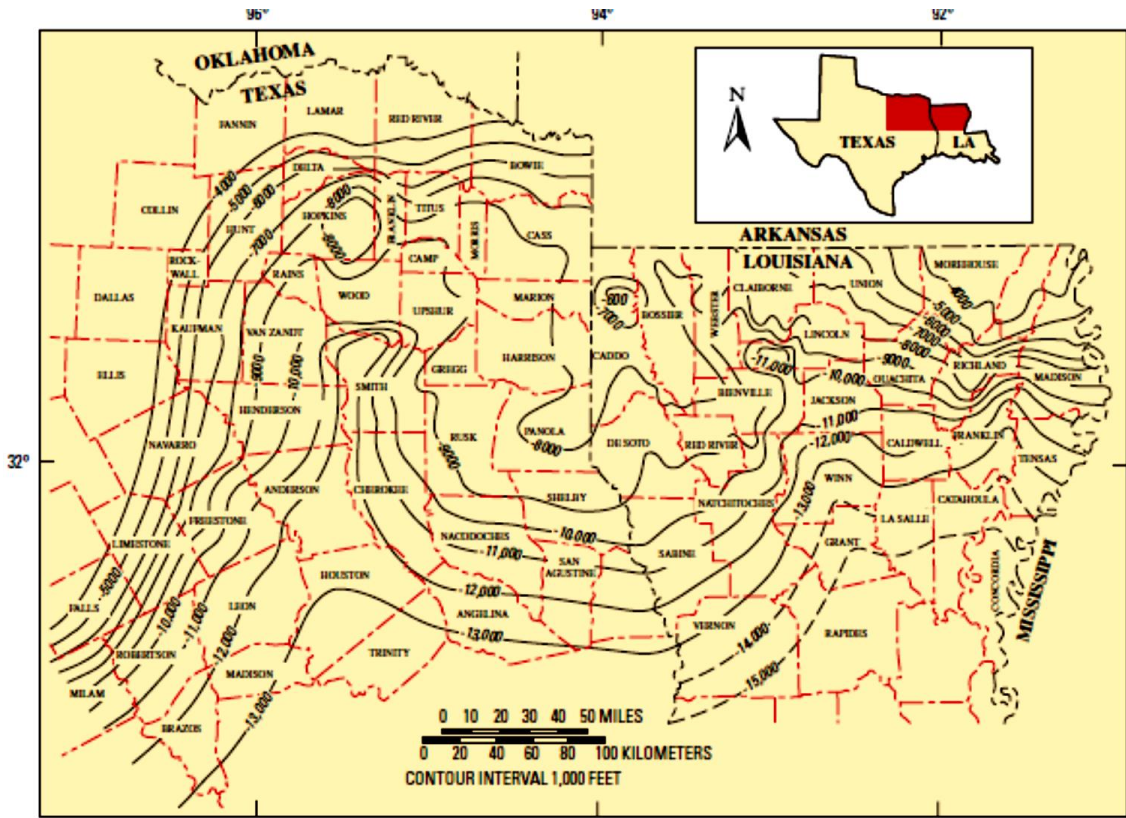


Figure 7–Structure, top of the Cotton Valley Group Sandstone (base of Travis Peak Formation), showing the location of this study (modified from (Finley, 1984)).

*Cotton Valley*: The Cotton Valley Group is an Upper Jurassic to Lower Cretaceous sequence of sandstone, shale, and limestone (Li, 2007). In the study area, the top of the Cotton Valley ranges from 4,000 ft below sea level in the updip zero region to more than 13,000 ft below sea level, is the downdip margin.

The Cotton Valley Group and overlying Travis Peak (Hosston) Formation represent the first major influx of terrigenous clastic sediments into the Gulf of Mexico Basin (Salvador, 1987). Prodelta, delta-front, and braided-stream facies have been identified in the Cotton Valley Group in the northwestern part of the East Texas basin (McGowen & Harris, 1984). The prodelta facies contains minor amounts of very fine-grained sandstone and siltstone (Li, 2007). Cotton Valley delta-front deposits typically consist of interbedded sandstone and mudstone with a few thin beds of sandy limestone, and commonly, they are overlain by a thick wedge of braided-stream sediments (McGowen & Harris, 1984)

In parts of East Texas, the Travis Peak / Cotton Valley boundary is marked by a regional transgressive deposit, the Knowles Limestone (Li, 2007). However, the Knowles Limestone does not extend throughout the East Texas basin (Saucier, 1985), and where it is absent, Travis Peak sandstones directly overlies Cotton Valley sandstones (Finley, 1984), making correlation of the boundary difficult to impossible.

- **Bossier Formation**: Throughout most of the East Texas, Bossier sequence is interpreted as marine shale. However, along the south part of the west flank, well-developed sandstone bodies are interbedded with the marine shale (Li, 2007). The top of Bossier is approximately 19,000 ft in the deep

(Li, 2007). Basinward deterioration of the Bossier reflector may be attributed to data quality changes in rock properties.

- *Shuler Formation*: They are composed of sandstones, siltstones and shales deposited in terrigenous, deltaic and nearshore marine environments (Dickinson, 1969). Deposits unconformably overly the Haynesville Formation and underlie the Hosston Formation and the Shuler Formation laterally grades into the Bossier Formation or Cotton Valley Sandstone (Foote, Massingill, & Wells, 1988).

*Travis Peak*: The Travis Peak ranges from alluvial fine-grained sands to fine gravels (Warner, 1993). The sandstones are fine-coarse grained, multicolored, rich in mica, and are lignitic; the shales and mudstones are multicolored, silty-sandy, rich in mica, calcareous and are fossiliferous. The Travis Peak Formation overlies the sands and shales of the Cotton Valley Group (Warner, 1993). Due to the presence of similar rocks, it is difficult to determine the contact of Lower Cretaceous Travis Peak and the Upper Jurassic Cotton Valley (Figure 6).

The top of the Travis Peak Formation is transitional and characterized by marine clastic sediments which grade up toward the Pettet Formation (Li, 2007). Bushaw (1968) mentioned that during early Travis Peak time, the study area was dominated by alluvial plane and shoreline environments. However, there was dramatic shift of land during late Travis Peak-Pettet which resulted in marine sedimentation. “The lower Travis Peak Formation is composed of thick fluvial channel-fill sandstones deposited by straight channels, braided streams” (Bushaw, 1968). In the middle and upper Travis Peak



Formation, sandstones are braided to meandering, channel-fill deposits that are interbedded with deltaic deposits (Tye, 1989).

A major sea level regression marks the end of the Cotton Valley age and the beginning of Travis Peak age (Vail & et al, 1977). The retreating sea plus an increase in uplift to the north and basin subsidence in the south resulted in extensive erosion in the coastal plains of the northern Gulf Coast and massive deposition of terrestrial-sourced clastic sediments in a marginal marine regressive environment (Warner, 1993). The depth of Travis Peak (Hosston) is shown in Figure (7).

*Sligo*: The Sligo Formation overlies the Hosston Formation (Figure 6). It is a gray-brown argillaceous and fossiliferous limestone (Warner, 1993). A period of continued sea level rise persisted in the Gulf Coast during the early Sligo (Vail & et al, 1977). A regressive sea sequence caused an end to the period of predominant Sligo carbonate deposition during the end of the Aptian Stage (Warner, 1993).

*The Rusk Formation/Glen Rose Formation*: Sedimentary patterns within these units indicate a major withdrawal of the seas which reached a regressive end during the deposition of the overlying Paluxy Formation (Nichols, 1964). A basal anhydrite member which was deposited in a mildly regressive environment was the part of basinal facies of the Rusk Formation (Foote, Massingill, & Wells, 1988) (Figure 6). In the upper part of the basinal facies are limestones which grade into updip sandstone facies and were deposited in a minor transgressive cycle. The Rusk/Glen Rose Formation in East Texas is composed of interbedded shales and limestones which were deposited in shallow marine environments and some thin strandline sandstones (Foote, Massingill, & Wells, 1988).

There is a regional tilt in the area in the northeast Texas which marks the close of the Trinity group in the Lower Cretaceous period.

*Pine Island:* This is the oldest formation of the Glen Rose Subgroup, and it is mostly a carbonate.

*James Lime:* The James Lime conformably overlies the Pine Island Formation. The top of the James Lime is picked at the base of the Rodessa (Warner, 1993) (Figure 6).

*Rodessa:* It conformably overlies the James Lime Formation and is the oldest unit of Trinity age. It can be difficult to identify in the northern Gulf Coast, because of the absence of Ferry Lake Anhydrite which separates similar rocks of the Mooringsport Formation (Warner, 1993). Based on log and sample data it can be identified as a gray, arenaceous–argillaceous, partly oolitic limestone containing fossil debris and is interbedded with thin, hard, fine-grained sandstone, brown granular dolomite, gray to brown red micaceous shale, and white to buff anhydrite stringers (Warner, 1993) (Figure 6).

*Ferry Lake:* The Ferry Lake Anhydrite is present to the south of the Wiggins Arch, and when present is a massive, white anhydrite interbedded with thin irregular lenses of gray shales, limestone and dolomite (Warner, 1993).

*Mooringsport:* Like the Rodessa Formation, it consists primarily of dark gray–reddish–brown, oolitic, fossiliferous limestones interbedded with dark gray shale, multicolored thin sandstone, marl, and thin irregular beds of anhydrite (Warner, 1993).

*Paluxy*: The Paluxy Formation conformably overlies the Mooringsport Formation. The shales are gray–dark gray, firm–hard, brittle, sandy and calcareous in part whereas, the sandstone is gray to tan, firm–hard to friable to unconsolidated, poorly sorted, calcareously cemented, and medium to very fine grained (Warner, 1993).

*Washita–Fredericksburg Group*: After the deposition of the Paluxy Formation, there was an advancement of the seas over northeast Texas. As a result, the Goodland Formation was deposited in a shallow-marine environment during a period of little sediment influx (Foote, Massingill, & Wells, 1988). Extensive porous facies is exhibited in the lowermost Goodland Formation which is formed in the extreme northeast corner of the basin (Eaton, 1956). In the shallow seas the Kiamichi Shale, which consists of fine grained terrigenous sediments got deposited over the basin (Rainwater, Regional Stratigraphy and petroleum potential of Gulf Coast Lower Cretaceous, 1970) (Figure 6). At the time of the deposition of the Washita Group, there were shallow marine seas which covered the East Texas basin and there prevailed a carbonate depositional environment over the area of the Angelina-Caldwell flexure (Foote, Massingill, & Wells, 1988). There were limestones deposited on the shelf at the north end of the basin and in deeper waters to the south, when there was little or no influx of the sediments. The carbonate formations from oldest–youngest are, the Duck Creek Limestone, Fort Worth Limestone, Weno-Paw Limestone, Main – Street Limestone, and Buda Limestone (Foote, Massingill, & Wells, 1988). As shown in Figure 6, there is an interval between the Duck Creek Limestone and the Main Street Limestone that is equivalent to the Georgetown Formation.

## ENGINEERING BEHAVIOR OF SANDSTONES

There have been many studies on sandstones showing the variation in their geomechanical properties. These variations are mainly due to differences in some petrographical characteristics which include grain size distribution, packing density, packing proximity, type of grain contact, length of grain contact, amount of void space, type and amount of cement/matrix material and mineral composition (Bell, 2007).

Bell & Culshaw (1998) demonstrated that sandstones with smaller mean grain size possessed higher strength. Sandstones having uniaxial compressive strength in excess of 40 MPa fall under the category of densely packed (Bell, 2007). UCS is a compressive strength of the material to withstand loads which has a tendency to reduce the size. The amount of grain contact was a major influence on the strength and deformability of sandstones (Dyke and Dobereiner, 1991). The cement content and interlocking of quartz grains was also considered to be important in terms of strength and it was also noted that with an increase in cement content there was an increase in the strength of the rock as the cement helps in binding the grains together (Bell, 2007).

The compressive strength of sandstones is also influenced by the porosity; the higher the porosity, the lower the strength of the sandstone (Bell, 2007). Moisture content contained by the sandstones is not an important factor in terms of strength because Hawkins & McConnell (1992) mentioned that sandstones with significant amount of clay minerals or rock fragments show loss in wetting, which is due to possible expansion of

clay mineral content. The testing of sandstones for indirect tensile strength showed that the values are almost 1/15<sup>th</sup> of their compressive strength (Bell, 2007).

Sandstone's degree of resistance to weathering depends on the mineralogical composition, amount and type of cement, porosity, type and amount of cement and lamination (Bell, 2007). Generally, sandstones contain quartz which is highly resistant to weathering, but the presence of other minerals like feldspar (which maybe kaolinized) and calcareous cement (which may react in the presence of weak acids) can make sandstone durability very weak (Bell, 2007). When tested for compressive strength, these type of sandstones which can be disaggregated when subjected to saturation have a compressive strength less than 0.5 MPa (Yates, 1992).

## UNIAXIAL COMPRESSIVE TEST

Uniaxial compressive strength ( $\sigma_c$ ) is generally known as the boundary between rocks and soil in rock mechanics and engineering geology, rather than rock texture, structure or weathering (Palmstrom, 2011). There are many classifications for compressive strength of rocks, which are presented below in Table 1. The uniaxial compressive strength of rocks can be determined from direct and indirect tests. Direct tests include laboratory methods, whereas indirect methods include point load tests. Point load tests are used to determine rock strength index.

Rock is defined as a naturally occurring material that consists of single or several minerals which can be held together by a matrix. The highest possible strength limit of a rock mass can be calculated from uniaxial compressive strength (Palmstrom, 2011). ISRM (1981) suggests that the uniaxial compressive strength calculated in an area should be given as the mean strength of the samples as determined away from faults, joints and other discontinuities to avoid weakness and weathering. When a rock sample is said to be anisotropic, the value of rock mass index should be tested towards the direction of the lowest mean strength and in such cases it is highly recommended to measure the uniaxial compressive strength in all directions (Palmstrom, 2011).

Laboratory testing for uniaxial compressive strength can be time consuming because it requires precision and accuracy (Figure 9). There are many tests which can be done in the field to save time, but they may not be accurate as compared to the laboratory

tests. The Schmidt hammer test can be used as an alternate to the laboratory test. Strength can also be assessed non-quantitatively if there is information on the rock like composition, anisotropy and weathering (Palmstrom, 2011).

Table 1 – Various strength classification of intact rock (Bieniawski, 1984).

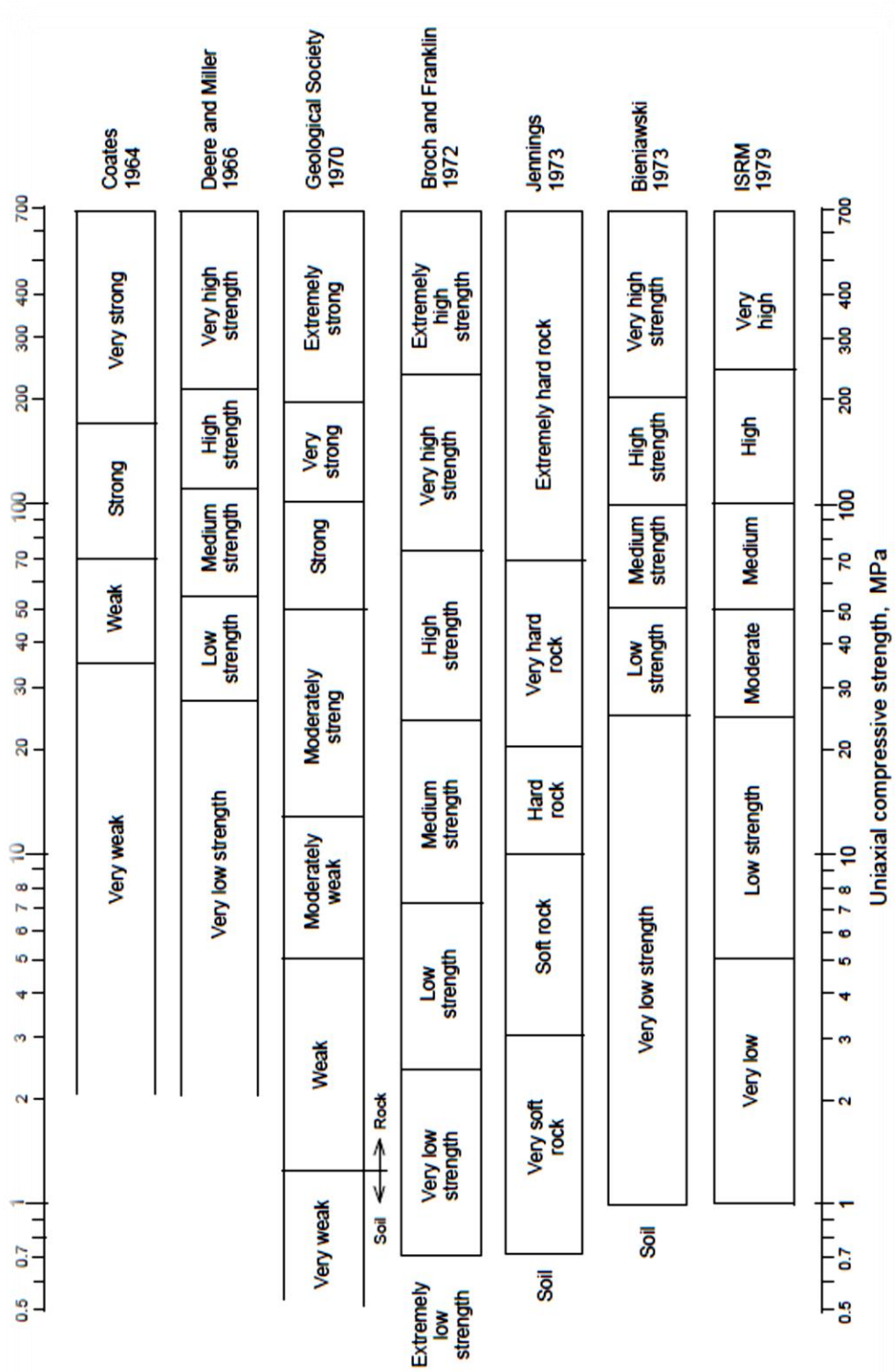






Figure 8 –Image showing the arrangement of Unconfined Compression test which can hold up to a core sample of NX size and in the center is the sample taken from a core which has a length to diameter ratio of 2 (Geocomp Corp, 2015).

### Point load test to determine compressive strength

Point load test is used to determine the rock's strength index. It is based on the principle of loading a rock in between two hardened steel ends. ISRM (1985) described this process in further detail. Bieniawski (1984) recommends this test very highly for strength testing, because point load strength index ( $I_s$ ) can be determined in the field using simple and portable equipment. Broch (1983) mentions the advantages of the point load test as it can be calculated without machined specimens and also the specimen's shape and size are considered for calculating the index of point load, even though the specimen has rough or smooth surfaces.

#### Point load strength index ( $I_s$ )

On the basis of tensile characterization of a rock and classification, the point load strength test is irrelevant even though it is considered as an indirect tensile test (ISRM, 1985). Strength classifications using the point load test are given in Table 2.

Table 2 – Various classifications of point load strength index ( $I_s$ ) after (Bieniawski, 1984).

Term	Point load strength index ( $I_s$ )
Very high strength	$I_s > 8$ MPa
High strength	$I_s = 4 - 8$ MPa
Medium strength	$I_s = 2 - 4$ MPa
Low strength	$I_s = 1 - 2$ MPa
Very low strength	$I_s < 1$ MPa

Broch (1983) mentioned that a strength anisotropy index ( $I_a$ ) can also be measured from maximum and minimum strength, which are parallel or perpendicular to weakness planes such as foliation, cleavage, etc (Palmstrom, 2011).

Correlation between point load strength and uniaxial compressive strength

Since the point load test is easy to measure and reliable in some cases it can easily replace uniaxial compressive tests (Palmstrom, 2011). Hoek & Brown (1980) mentioned that uniaxial compressive strength is a function of point load strength and is calculated from the formula:

$$\sigma_c = k \times I_s \quad (1)$$

Here k is constant value which generally ranges from 15 to 25 and in some cases between 10 to 50 for anisotropic rocks (Palmstrom, 2011). Research by various authors has refined this constant as described classification in Table 3.

Table 3 – Various classification of k after (Palmstrom, 2011), where D is diameter.

Authors reference	k value
Franklin (1970)	k = approx. 16
Broch & Franklin (1972)	k = 24
Indian Standards (1998)	k = 22
Hoek & Brown (1980)	k = 14 + 0.175D
ISRM (1985)	k = 20 – 25
Brook (1985)	k = 22

Ghosh & Srivastava (1991)	k = 16
---------------------------	--------

### Compressive strength from Schmidt Hammer test

A non-destructive way to approach a compressive test is by performing a Schmidt Hammer test which measures the rebound hardness of a rock (Palmstrom, 2011). It is based on the principle that a plunger is released by a spring and it hits the surface of the rock; the distance of rebound is measured numerically by a scale (Palmstrom, 2011).

Ayday & Goktan (1992) mentioned that the Schmidt Hammer measures rock properties which are based on elastic impact of two bodies, one of which is impact by the hammer and the other is impact at the surface of the rock. To measure this impact there are two types of Schmidt Hammer, they are L and N type Schmidt Hammers shown in Figure 8 and 9 respectively. These hammers are designed on the basis of impact energy and the L type Schmidt Hammer has an impact energy of 0.735 N/m, which is 1/3<sup>rd</sup> of the N type (Palmstrom, 2011). ISRM (1978) suggested that the L type Schmidt Hammer can be used for measuring uniaxial compressive strength of rocks which are in the range of 20-150 MPa.



Figure 9 –L type Schmidt Hammer, where A is the needle which is placed at the surface of the rock and B is the scale of the hammer which is used to measure the strength in MPa (Proceq, 2016).



Figure 10–N type Schmidt Hammer, where A is the needle which is placed at the surface of the rock and B is scale of the hammer which is used to measure the strength in MPa (PCTE, 2016)

### Field Tests To Identify Compressive Strength

The strength of the rocks can be assessed sometimes by using simple field techniques (Palmstrom, 2011). Based on factors like the hardness of rock, tests for uniaxial compressive tests can be carried out in the field itself. Table 4 below shows a general classification of compressive strength based on simple tests done in the field.

These test can be made using a common geological hammer; rock samples should be at least 10 cm thick and placed on a hard surface. Tests made with one's hand should be made on pieces which are 4 cm thick (Palmstrom, 2011). These pieces should not contain cracks; in different directions of the rock anisotropic tests should be made (Palmstrom, 2011).

Table 4 – Compressive Strength of rocks from field identification (ISRM, 1978)

Grade	Term	Field Identification	Range of UCS (MPa)
R0	Extremely Weak Rock	Intended by thumbnail	0.25 – 1
R1	Very Weak Rock	Crumbles under firm blows of geological hammer; can be peeled by a geological knife	1 – 5
R2	Weak Rock	Can be peeled by a geological knife with difficulty; shallow identifications made by firm blow with point of geological hammer	5 – 25
R3	Medium Strong Rock	Cannot be scraped or peeled by pocket knife; specimen can be fractured with single firm blow of geological hammer	25 – 50
R4	Strong Rock	Specimen requires more than one blow of geological hammer to fracture	50 – 100
R5	Very Strong Rock	Specimen requires many blows of geological hammer to fracture	100 – 250



R6	Extremely Strong Rock	Specimen can only be chipped with geological hammer	>250
----	--------------------------	--	------

## TENSILE STRENGTH

Tensile strength is an important property for the strength of a rock because it tells the vulnerability of the rock towards tensile failure when a load is applied on it (Building Research Institute, 2016). This test usually results in low strength as compared to the uniaxial compressive strength test because tensile strength is applied towards the minimum stress direction, whereas uniaxial compressive strength is applied towards the maximum stress direction possible. Tensile strength is determined by indirect methods like 1) Splitting Tensile Test and 2) Flexure Test.

### Splitting Tensile Test

ASTM (D 3967-95a) has published a standard procedure for how to test a rock for splitting tensile strength. The general procedure is to take a sample of NX size, where N could be any number and X is any unit associated with it. The sample is placed horizontally in between the loading surface of a compression testing machine (Figure 12). A load is applied uniformly along the length of the rock sample until it reaches failure.

As the failure is achieved the sample is split into two halves along the vertical plane because of the indirect tensile stress which is generated due to Poisson's effect (Building Research Institute, 2016). "Poisson's effect is based on the ratio of transverse contraction strain to longitudinal extension strain in the direction of stretching force" (Lakes, 2016). Two types of stresses, horizontal and vertical, are developed in this testing when the compression load is applied (Figure 13). When the loading is applied it is

estimated that the compressive stress is acting for about  $1/6^{\text{th}}$  of the depth and the remaining is under tension due to poisson's effect (Building Research Institute, 2016).

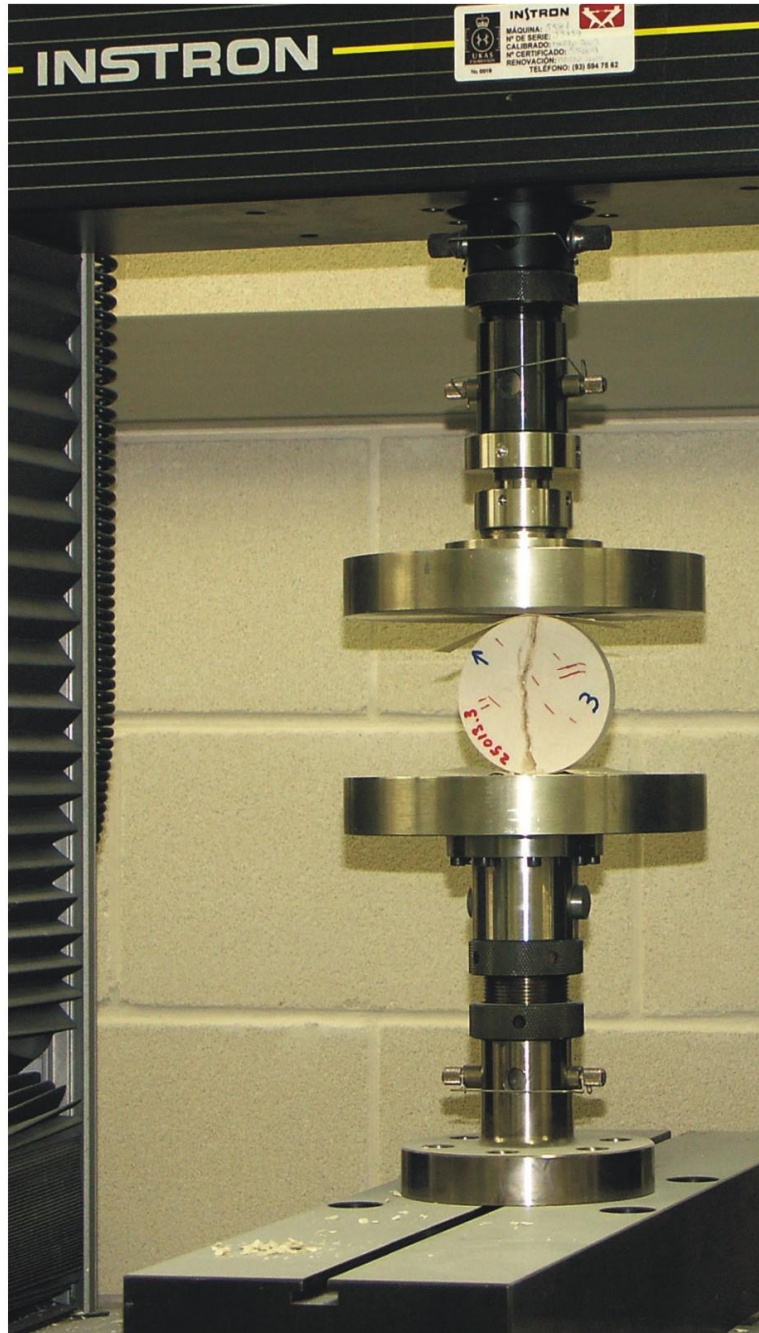


Figure 11 – Image showing the arrangement of Tensile strength, which can also hold up a core size of NX size, and a length to diameter ratio of 4 or 5 (Istone, n.d.)

breins

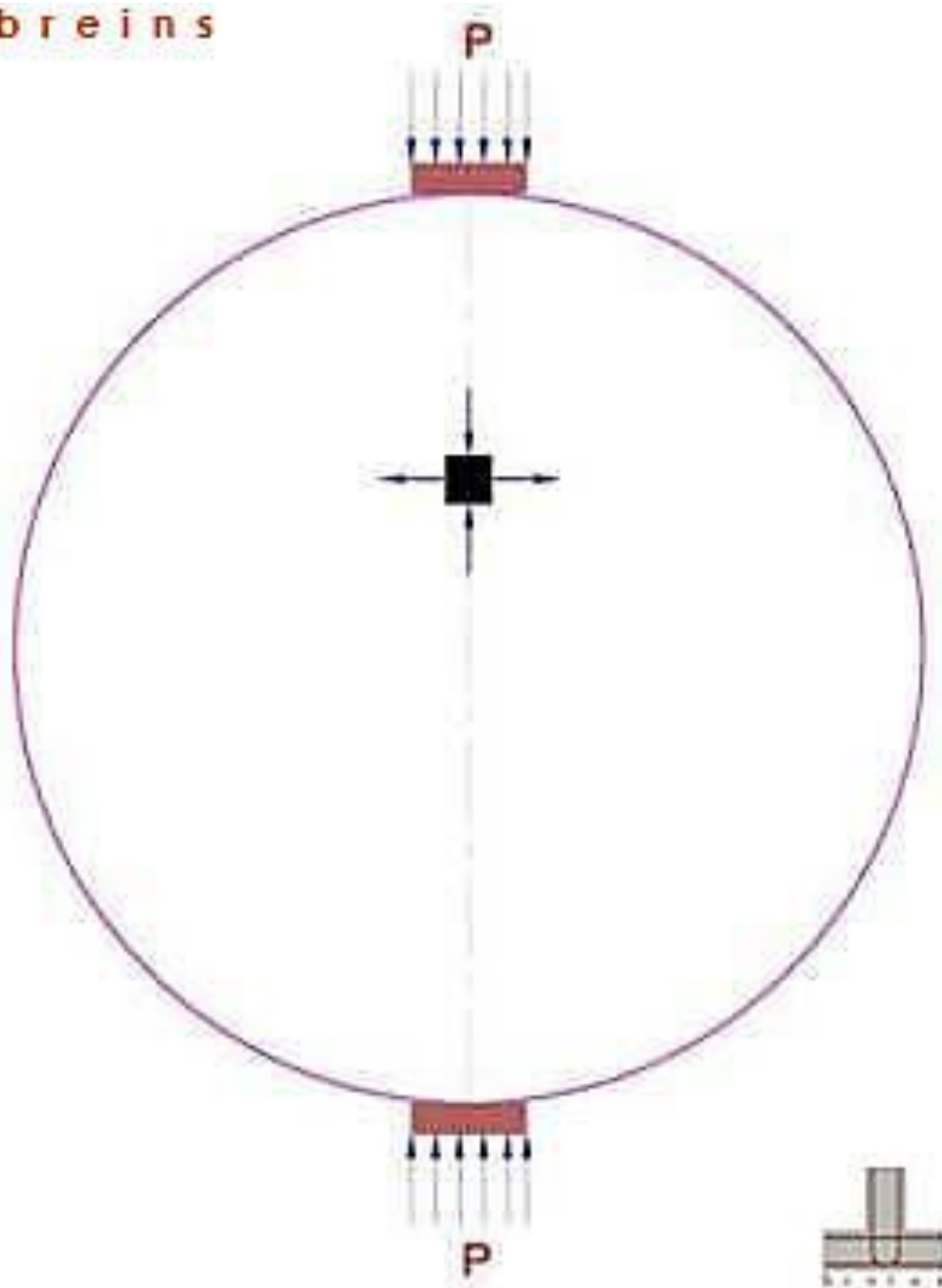


Figure 12 – Horizontal and Vertical stresses measured from Splitting tensile test (Building Research Institute, 2016).

## Flexure Test

This is the second most common indirect test done to determine tensile strength. Generally, it is done for hard rocks or concrete. ASTM D1635 has mentioned general guidelines to complete the testing. The sample is located at 1/3<sup>rd</sup> of the distance between two span points. The standard size of the specimen is 150 x 150 x 750 mm (Building Research Institute, 2016).

The arrangement is shown in Figure 12. The principle for this test is based on loads applied equally at a distance of 1/3<sup>rd</sup> from the bottom of the supporting beam (Building Research Institute, 2016). Loading is increased with an increase in stress in the range of 0.02 MPa and 0.10 MPa with the lower rate for low strength rock/concrete and the higher rate for high strength rock/concrete (Building Research Institute, 2016).

Based on this test, the beam bends at 1/3<sup>rd</sup> of the area between the applied load and no shear force is applied in this area, hence it is the area where maximum pure bending is induced by a shear force of zero (Building Research Institute, 2016). Maximum tensile stress is reached when a fracture occurs within the middle 1/3<sup>rd</sup> of the beam with an increase in load; this is called modulus of rupture  $f_{bt}$ , which is calculated by:

$$f_{bt} = Pl \div bd^2 \quad (2)$$

Where, P = load at failure

l = beam span between supports

d = depth of beam

b = width of beam;  $f_{bt}$  = modulus of rupture

## METHODOLOGY

### Sample Preparation and testing

The main aim of this study is to determine the mechanical properties of core samples from the Travis Peak Formation. Core samples were selected from Stephen F. Austin State University's Core Lab Repository and testing for geotechnical properties was done at the University of Houston. Standard samples were prepared from the selected cores. The experimental work is mostly based on measuring the load, at the point which the rock is subjected to stress for both uniaxial compressive strength and tensile strength tests (Baykasoğlu, Güllü, Çanakçı, & Özbakir, 2008). All the procedures were based on guidelines from ASTM D 2938-95 and ASTM D 3967-95a. A total of 12 samples were subjected to the testing procedure (Table 6).

The UCS test was measured in accordance with ASTM D 2938-95 guidelines. ASTM is American Society of Testing and Materials, an organization which is associated for publishing testing standards. ASTM D 2938-95 is a standard publication which deals with the testing of UCS and also the equipment and preparation of samples. Samples should have a size ratio of length to diameter of 2:1 for NX size core samples. N is also referred to any size of the core and X is any unit associated with it. If the sample's length to diameter ratio is not 2, then a correction value is applied (ASTM D 2938-95). For determining tensile strength, the sample size has to be of uniform thickness and width

and 2 inches longer than the gauge length (ASTM D 3967-95a). Sample width should not be less than 5mm, or greater than 25.4mm. Core samples were from the Travis Peak Formation and were prepared based on the above procedures.

The samples were divided into two sets, one for testing uniaxial compressive strength (UCS), and the other for testing tensile strength (Figure 14). Samples prepared for UCS require a base and top to be flattened, which was done by adding Sulfur melted at 300°F, then let it cool down to solidify and place in the instrument for measuring the load. Similarly, before working on the tensile strength, all the other parameters that were used for uniaxial compressive strength were conducted (Figure 15).

Uniaxial compressive strength was tested based on the information from ASTM D 2938-95. Experiments were performed after cutting the edges of the core samples. The ends were made flat and perpendicular to the axis of the samples so that loads were applied uniformly (Çanakçı, Baykasoğlu, & Güllü, 2009). Tensile strength values were determined indirectly from the Splitting Tensile strength method which was based on ASTM D 3967-95a. Samples were prepared from the cores. Splitting Tensile strength was used to test the tensile strength when a cylindrical specimen was subjected to failure, along the length of specimen under a certain load. The strength classification is given in the Table 5.



Table 5 – Strength classification of intact and jointed rocks (Ramamurthy & Arora, 1993).

<b>Class</b>	<b>Description</b>	<b>UCS (Mpa)</b>
<b>A</b>	Very high strength	>250
<b>B</b>	High strength	100-250
<b>C</b>	Moderate strength	50-100
<b>D</b>	Medium strength	25-50
<b>E</b>	Low strength	5-25
<b>F</b>	Very low strength	<5

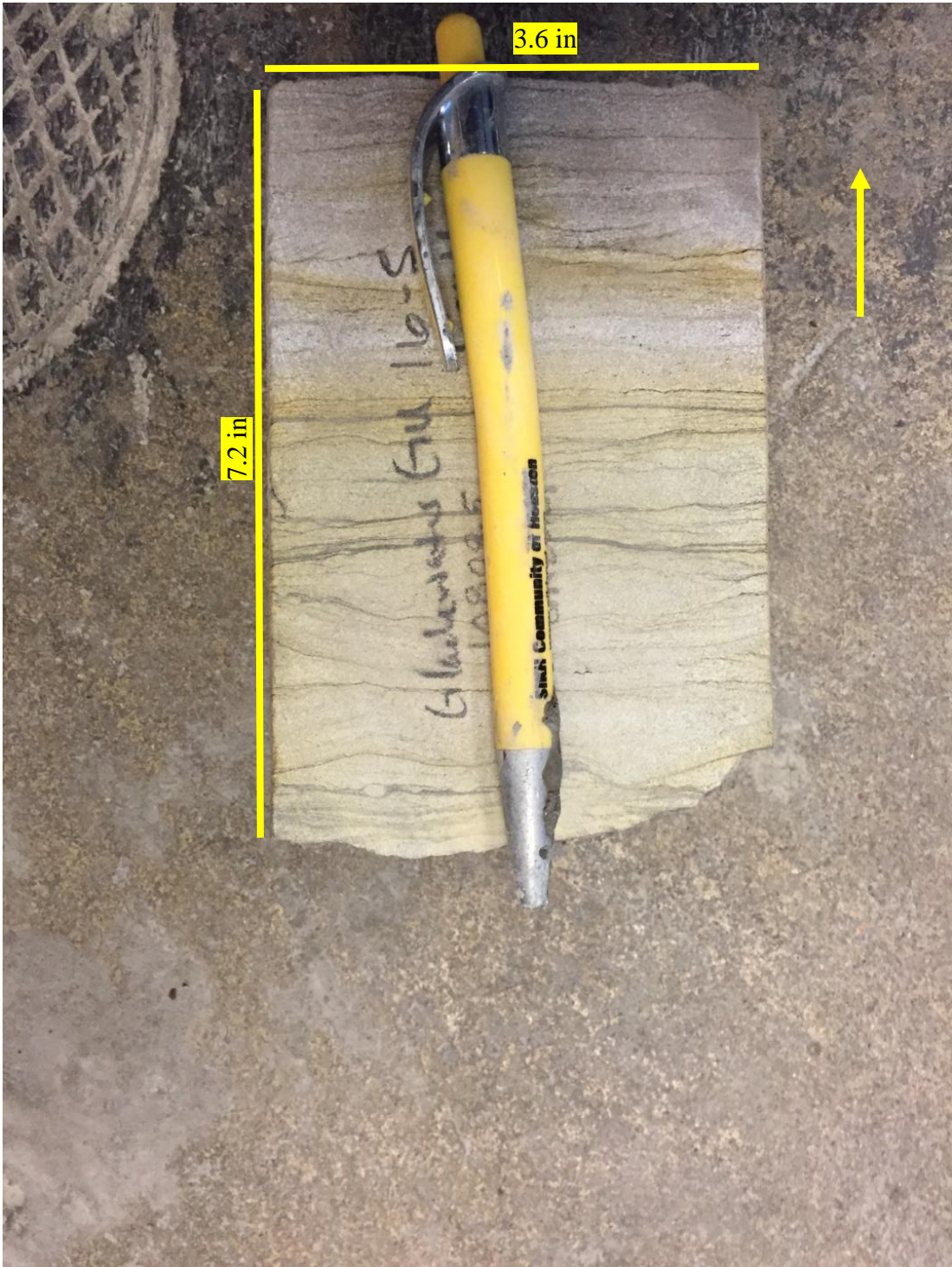


Figure 13–Image showing a core rock sample which was tested for UCS and Tensile strength which was cut into dimensions of 3.6 in width and 7.2 in length.



Figure 14—Equipment used for testing the compressive strength and tensile strength at University of Houston’s Civil Engineering Laboratory. The same equipment is used to test the UCS and Tensile strength and the samples are rested on the instrument depending upon the test and the load is applied.

## Regression Analysis

Regression analysis can be used to model, examine and predict different relationships. Why would one use regression analysis? In the view of earth sciences, regression analysis offers a mathematical relationship between two or more variables (Maher Jr., 2016). This relationship can be further used to predict one variable from the known variable.

A linear regression equation is given by the formula  $y = mx + c$ , where  $c$  is the  $y$  intercept and  $m$  is the slope of the given line (Figure 20). Linear equations can be positive or negative, based on the value of slope (Figure 21). The default convention that goes with regression analysis is that  $x$  represents the independent variable and  $y$  represents the dependent variable (Maher Jr., 2016). The predictions of the values of  $y$  are made through the values of  $x$ . The dependent variable is sometimes also called a criterion variable, endogenous variable, prognostic variable, or regressand and the independent variable is called exogenous variable, predictor variables or regressors (Statistics Solutions, 2013).

Linear regression involves more than just fitting a line through a set of data points. This includes a three step process, which is 1) analyze and correlate the data, 2) estimate the model, which includes the best fit line, and 3) evaluate the usefulness of the model (Statistics Solutions, 2013).

Regression analysis is used for three major purposes. First is the casual analysis, second is to forecast an effect and third is to forecast a trend (Statistics Solutions, 2013). Casual analysis is used to identify the strength of the effect that the independent variable has on a dependent variable. A change in a dependent variable, when subjected to change in the independent variable, deals with forecasting an effect. Trend forecasting is used to predict trends and future values.

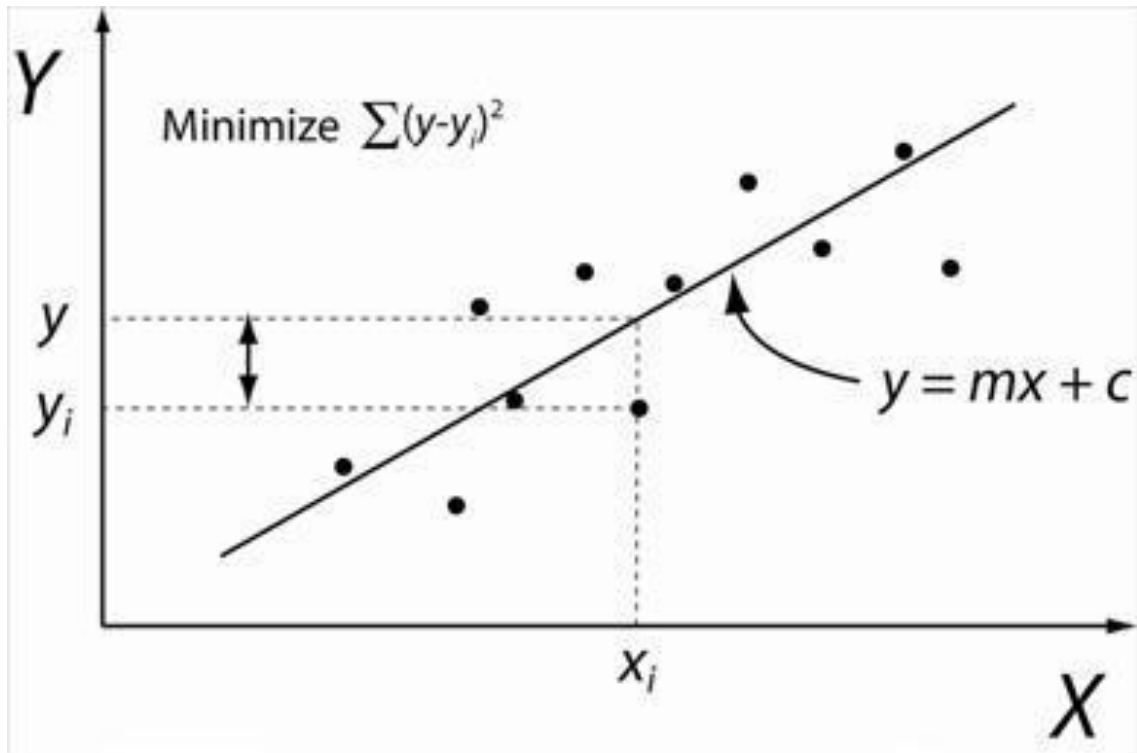


Figure 15–Image showing the equation for the linear regression analysis and the trendline (University of Washington, 2016).

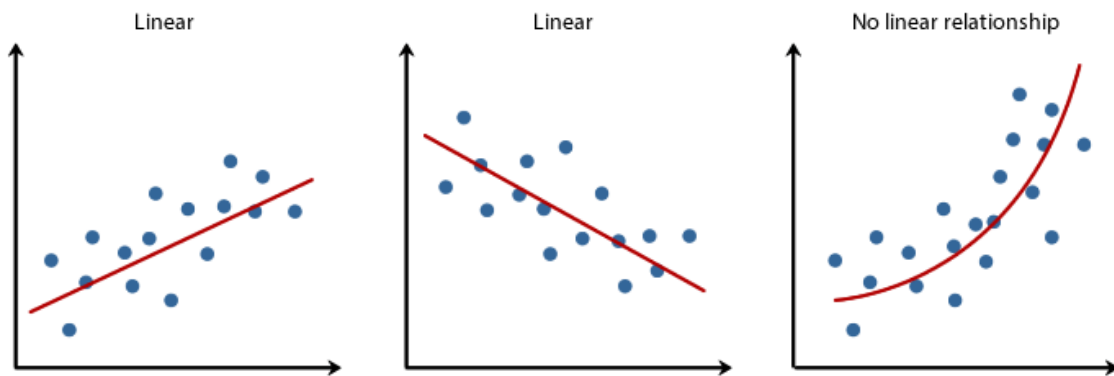


Figure 16–The above figure shows three different types of linear regression equations. First image shows a positive trend of the linear equation which has a positive slope. Second one shows a negative trend of the linear equation which has a negative slope. Third one is a non-linear equation (Laerd Statistics, 2016).

Linear regression can be of two types. First is bivariate regression or simple regression is associated with one dependent variable and one independent variable. Second is multivariate or multiple linear regression. It is associated with more than 2 independent variables and one dependent variable. In this study a simple regression or bivariate regression is used to conduct the statistical analysis.

### Independent variables and Dependent variables

Regression equation is the mathematical formula which is applied to the different variables, so that the dependent variable can be predicted and a model can be estimated (ESRI, 2016). Unlike in geosciences, where x and y are used as coordinates, here in regression they are denoted as independent and dependent variables respectively. There is a regression coefficient associated with the independent variable which describes the strength and sign of the variable's relationship to the dependent variable (ESRI, 2016). A typical regression equation looks like as shown below:

$$y = \beta x + \varepsilon \quad (3)$$

Where,

y = dependent variable

$\beta$  = coefficient

x = independent variable

$\varepsilon$  = Random Error Term

Dependent variable (y) – This variable represents the process which is to be predicted. In the regression equations, they are shown on the left-hand side. To predict the value using dependent variable, a set of known y values are used to build the regression model and the known y values are referred as observed values (ESRI, 2016).

Independent variable (x) – This variable is used to predict the variable value of the model. In a generalized regression equation, they are placed on the right-hand side. From the equation (3), it can be inferred that dependent variable is a function of independent variable.

Regression coefficient ( $\beta$ ) – This is the value which is estimated from the regression tools. This value is for independent variable, which represents the strength and type of relationship between independent and dependent variable (ESRI, 2016). The coefficient is associated with positive sign, when the relationship is positive and vice-versa.

P-Values – Regression methods perform statistical tests to measure the significance of a coefficient by using a p-value. Null hypothesis for statistical tests shows that a coefficient is not significantly different zero (ESRI, 2016). Small p-values reflect small probabilities, which suggest that coefficient is important to the model, whereas coefficient estimates with near zero values do not help in predicting the model and are removed from the regression equations (ESRI, 2016).

$R^2$ /R-squared – R-squared and adjusted R-squared values are both derived from the regression equation to check the performance of the model. The value of R-squared



ranges from 0 to 100 percent, R-squared is 1.0 when the model fits perfectly and there is no error (ESRI, 2016). However, this happens in the case when a prediction is made of a form of  $y$  to predict  $y$ . A scatterplot showing the estimated and predicted values can be very useful in understanding the R-squared values. Adjusted R-squared is always less than R-squared because it reflects the complex number of variables (ESRI, 2016).

Residuals – They are the unexplained portion of the dependent variable, shown in the regression equation as  $\epsilon$ . Using values which are known for dependent variables and independent variables, regression equation will predict  $y$  values (ESRI, 2016). Residuals are also known as the difference between the observed  $y$  values and predicted  $y$  values. Large values of residuals indicate a poor fit.

Regression model is a process which deals with an iterative process, which involves finding an effective independent variable to explain the model and then removing the variables which are not good for the model (ESRI, 2016).

## RESULTS

### Uniaxial Compressive Strength

Core rock samples from the Travis Peak Formation in East Texas were used in this study. A map showing the location of the samples is shown in Figure 5. Cores selected for testing were half core rock samples. An extensive investigation was carried out to select the sandstone blocks of core samples from the Travis Peak Formation. Samples were selected carefully from the Stephen F. Austin State University's Core Lab Repository (Figure 14).

During the experimental work, the load for uniaxial compressive strength was calculated from the compressive strength instrument at University of Houston's Department of Civil Engineering Laboratory (Figure 15). Overall 12 samples were tested for uniaxial compressive strength. All the tests were followed under the specifications of (ASTM D 2938-95).

The samples were cut by a saw. All the samples were from NX size, where N was 4 inches. The height to diameter ratio was 2. In order to make the samples flat, they were layered with Sulfur melted at 300° F (Figure 22). As per norms of (ASTM D 2938-95) the sample was placed vertically under the instrument and tested until it reached failure by breaking; this is the point where the stress is maximum  $\sigma_1$  (Figure 23). The load was calculated in poundsforce (lbf).

Uniaxial compressive strength was calculated from the formula:

$$UCS \left( \frac{lbf}{in^2} \right) = \frac{Load (P \text{ in } lbf)}{Area (inches^2)} \quad (4)$$

Then uniaxial compressive strength was converted to SI Units by  $1 \text{ lbf/in}^2 = 6.894$  KPa.

All the calculated UCS are shown in the Table 7.



Figure 17–Top and bottom of the samples are flattened by adding Sulfur which is melted at 300° F. Cores are made flat so that they are stable when subjected to stress.

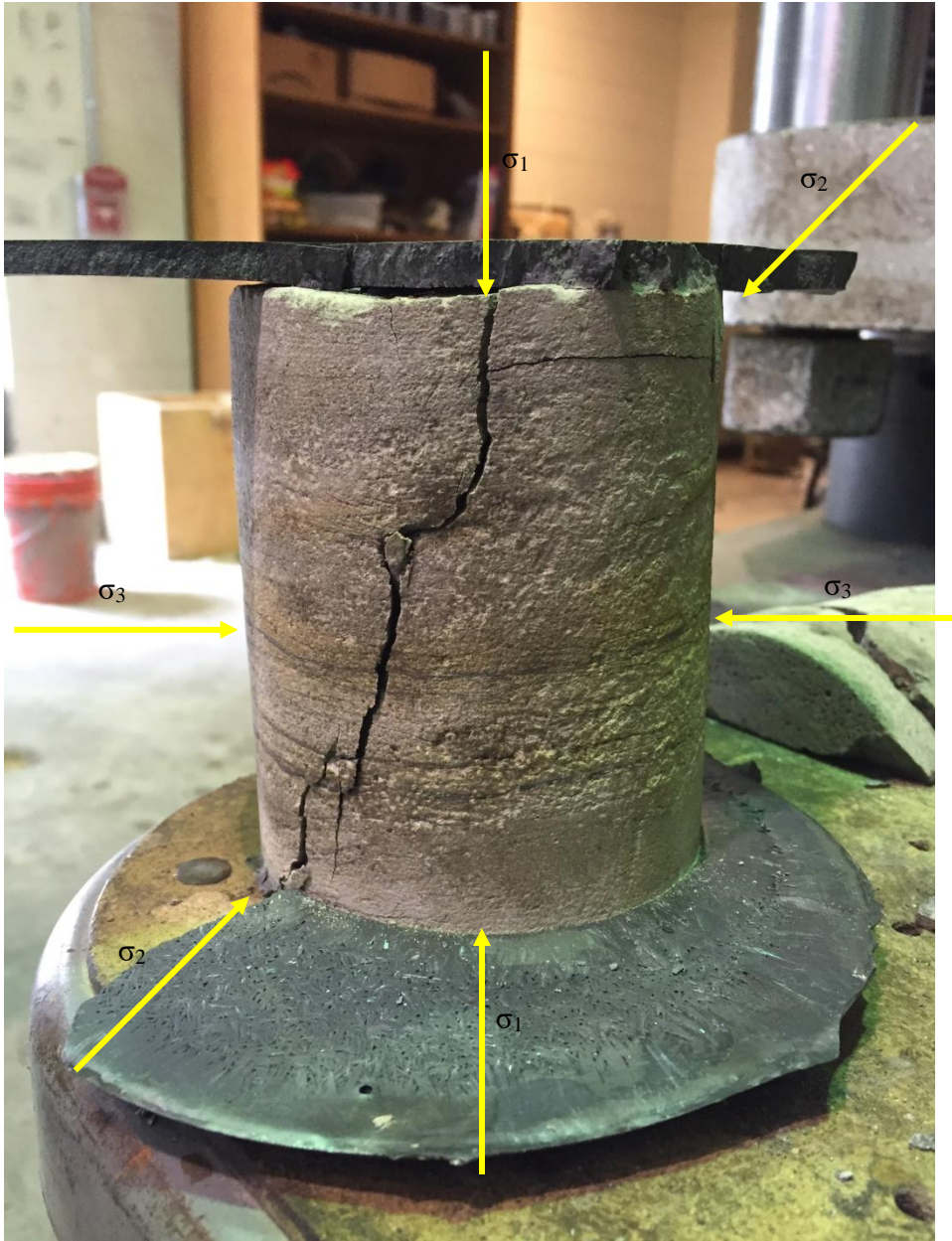


Figure 18—Failure from the maximum stress plane ( $\sigma_1$ ) results in the uniaxial compressive strength test. In this figure the three different stress planes are shown which are associated with uniaxial compressive strength. This image is captured after the UCS has been achieved.

The uniaxial compressive strength test of the samples has a range between 13.23 and 45.87 MPa with an average value of 27.43 MPa and standard deviation of 9.47. A frequency distribution histogram is plotted for the uniaxial compression strength, which shows major population in the range of 28.23 and 43.23 MPa (Figure 24). It also shows a nearly normal distribution of the samples. Based on the frequency and mean the rocks can be classified as medium strength (Table 5).

## Tensile Strength

Core rock samples of the Travis Peak Formation in East Texas were collected from Stephen F. Austin State University core lab repository (Figure 15). An experiment of splitting tensile strength was completed at University of Houston's Department of Civil Engineering Laboratory (Figure 14). These cores were measured for splitting tensile strength using the same instrument which measured compressive strength.

Twelve samples were tested for splitting tensile strength. All the tests were followed under specifications from (ASTM D 3967-95a). The samples were prepared first by cutting with a saw. Samples of NX size were used, where N is 4 inches and the height to diameter ratio was 2.

The samples were placed horizontally under the instrument compression was applied and testing was stopped when the rock broke from the area where minimum stress was applied,  $\sigma_3$  (Figure 25). The load was measured from the instrument in pounds\*force (lbf).

Splitting tensile strength was calculated from the formula:

$$T = \frac{2P}{\pi DL} \quad (5)$$

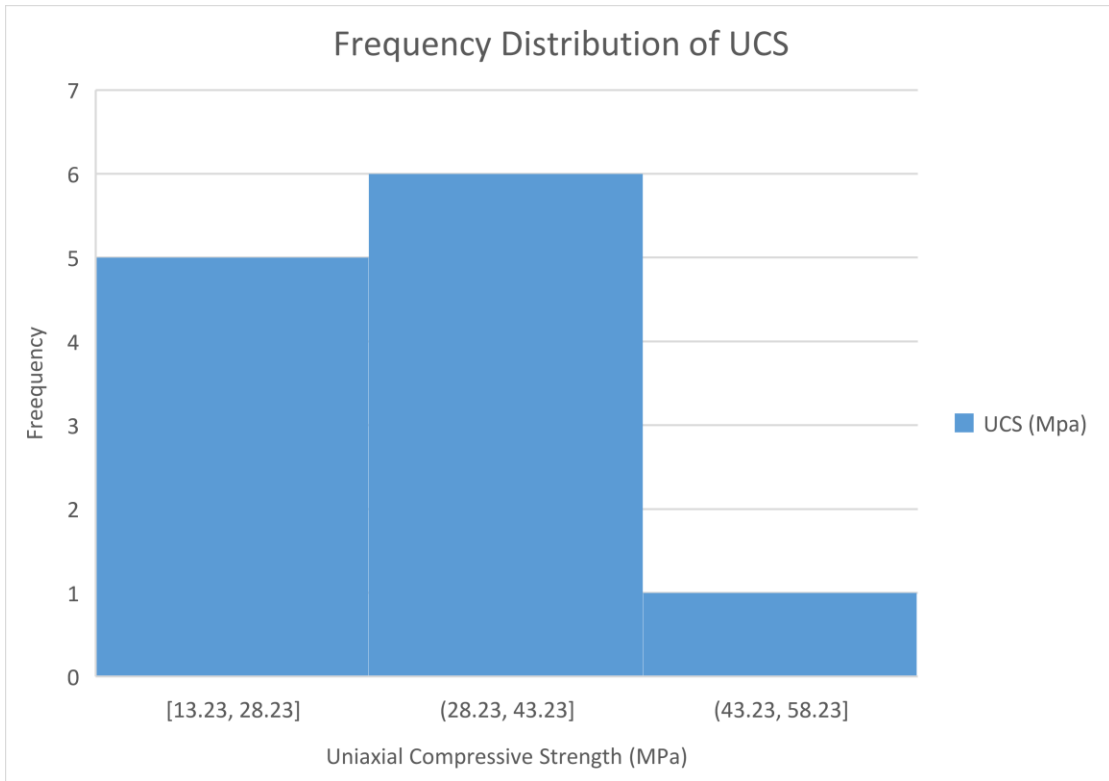


Figure 19–A plot showing the frequency histogram for UCS with the maximum number of 6 samples lie in the range of 28.23 to 43.23 MPa and minimum number of 1 sample lying in the range of 43.23 to 58.23 MPa.



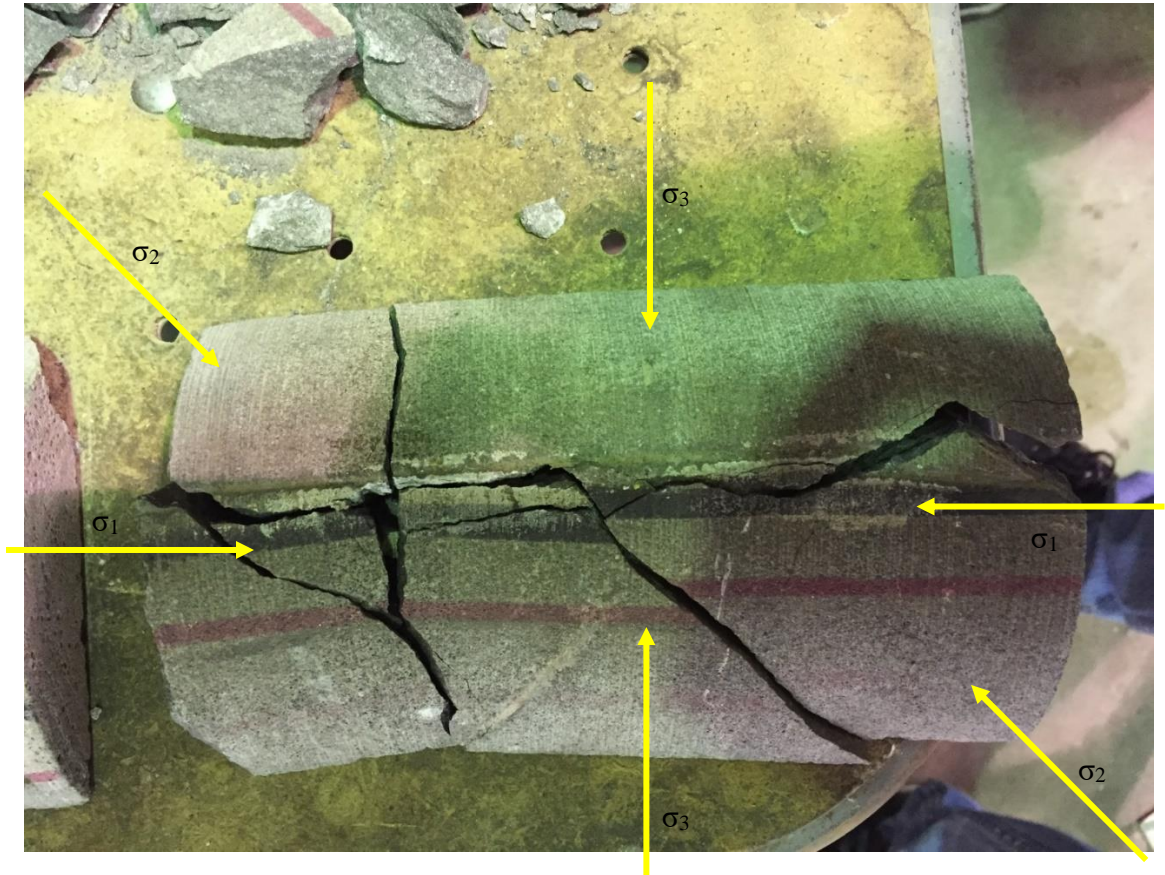


Figure 20—Failure from minimum stress plane ( $\sigma_3$ ) results in tensile strength. Three different stress axes associated with the tensile strength are shown in this figure. Figure is captured after tensile strength has been achieved.

Where T is tensile strength in lbf/in<sup>2</sup>, P is load applied in lbf, D is diameter of the sample in inches and L is the length of the sample in inches.

Splitting tensile strength was converted to SI units (MPa) by  $1 \text{ lbf/in}^2 = 6.894 \text{ KPa}$ . The calculated tensile strength is shown in the Table 7.

The tensile strength of the samples had a range between 1.69 MPa and 6.32 MPa with an average value of 3.97 MPa and standard deviation of 1.25. A frequency distribution histogram was plotted, which shows major population in the range of 3.59 and 5.49 (Figure 26). This also shows a near normal distribution of the samples. Hsu & Nelson stated that tensile strength is not valid for soft rock based on the theory of brittle failure, but compressive strength shows that the rock is of medium strength.

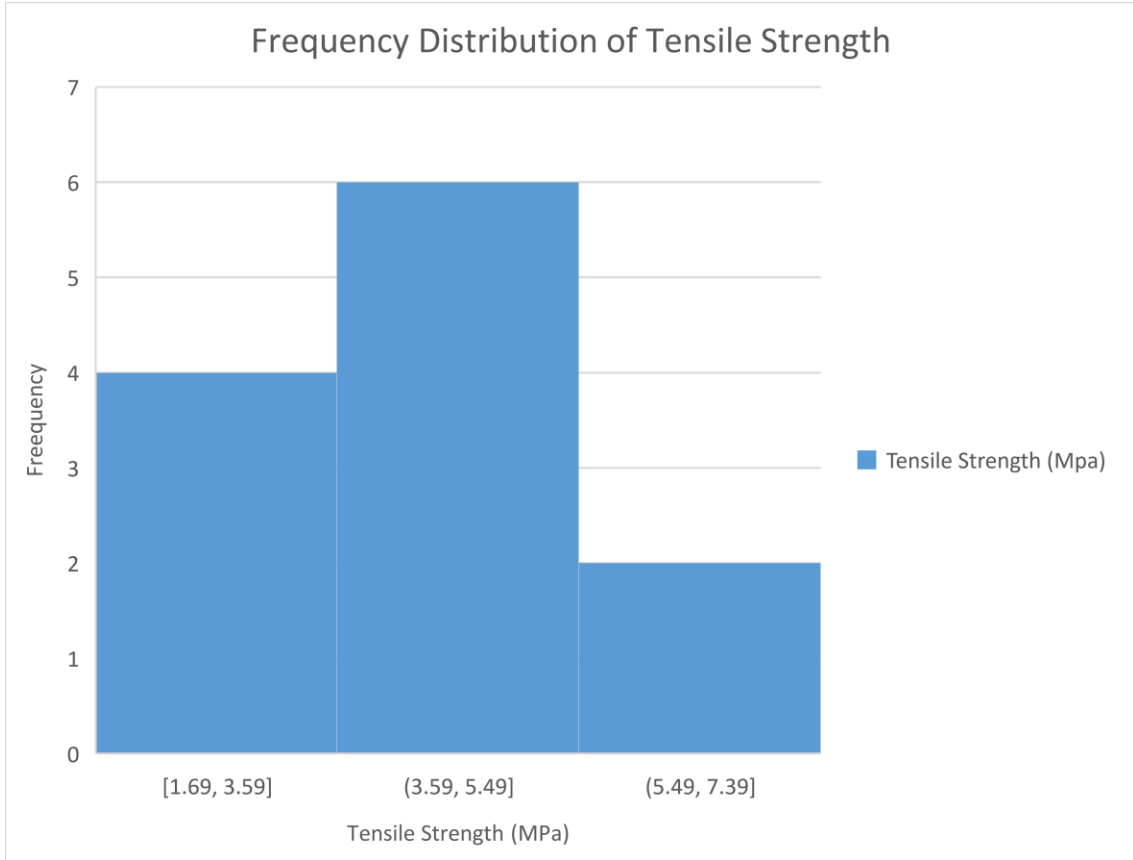


Figure 21—A plot showing the frequency histogram for Tensile strength, where the maximum number of 6 samples lying in the range of 3.59 to 5.49 MPa and a minimum of 2 samples lying in the range of 5.49 to 7.39 MPa.

## Regression Analysis

### Uniaxial Compressive Strength vs Tensile Strength

A simple regression analysis was calculated to relate uniaxial compressive strength and tensile strength. The data which are shown in Table 6 are used in the regression analysis approach. The input variable is the load for uniaxial compressive strength ( $X_1$ ) and the output variable is tensile strength ( $Y_1$ ). The equations which are obtained from the analysis were used in predicting the UCS values. Matlab software was used to carry out the simple linear regression analysis.

Regression equations obtained from the analysis are shown below:

$$Y_1 = 0.1005 \times X_1 + (1.293) \quad (6)$$

R – square of the predicted uniaxial compressive strength from the regression analysis is 0.6378. The test results of the simple regression analysis are shown in Figure (22).

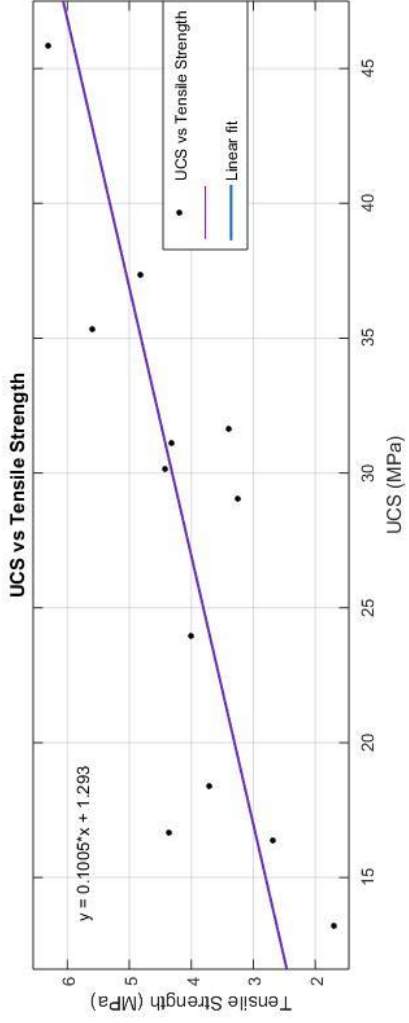


Figure 22–A plot showing linear regression analysis between Uniaxial Compressive Strength and Tensile strength which has a R-square value of 0.6378.

## Box Plots

Box plots are one of the tools which are used for depicting location and changes in information among data sets, particularly to see changes in variation among different groups of data (Chambers, Cleveland, Kleiner, & Tukey, 1983). The vertical axis in a box plot represents the response variable and the horizontal axis is the factor of interest. A box plot is completed by calculating the median and quartiles; the lower quartile is the 25<sup>th</sup> percentile and the upper quartile is the 75<sup>th</sup> quartile (NIST, 2016). A box plot is drawn when a symbol is placed at the median which is in between the lower and upper quartiles; this is the main body of the data and a line is drawn from the lower quartile to the minimum point and another from the upper quartile to the maximum point (NIST, 2016).

There are four major points in a box plot. The first point is the minimum point; the second point is the difference between the lower quartile and the minimum point; the third point is the difference between the upper quartile and the lower quartile and the fourth point is the difference between the maximum point and the upper quartile. The reason for using a box plot is to determine if a factor has a significant effect on the response with respect to either location or variation (NIST, 2016).

Box plots showing the variation in UCS and Tensile strength are shown in Figure (28).

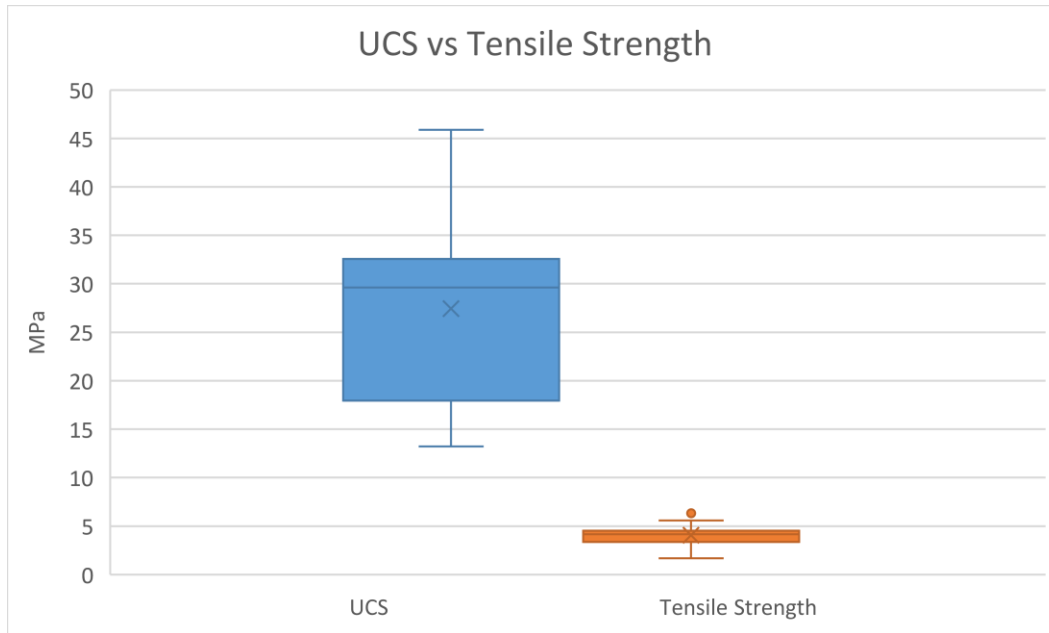


Figure 23–Box plot showing the difference in the values between UCS and Tensile strength. The y–axis is strength in MPa.

The orange dot is considered an “outlier” because it is more than 1.5 times the interquartile range larger than the third quartile. Interquartile range is calculated by  $Q3 - Q1$ . Below are the values represented by the box plot.

	UCS	TS
Min	13.23	1.69
Q1	17.9475	3.365
Median	28.23833	3.88
Q3	31.375	4.345
Max	45.87	6.32

Samples	UCS Load (lbf)	Tensile Load (lbf)	Area (square inches)	UCS (lbf/in <sup>2</sup> )	Tensile Strength (lbf/in <sup>2</sup> )	UCS (Mpa)	Tensile Strength (Mpa)
1	27580.42	13194.05	7.94	3473.6	1057.88	23.95	4.01
2	38623.84	15049.72	7.13	5417.09	1343.75	37.35	4.83
3	38511.99	15295.28	8.8	4376.36	1106.51	30.17	4.42
4	32720.08	10602.34	7.94	4120.92	850.01	31.63	3.4
5	47435.12	20798.41	7.13	6652.89	1857.04	45.87	6.32
6	37741.43	14603.07	8.36	4514.53	1112.03	31.12	4.32
7	33458.2	12849.63	8.8	3802.07	929.58	18.38	3.71
8	26473.15	10713.04	7.94	3334.15	858.96	29.05	3.26
9	16927.49	8345.24	7.13	2374.12	745.13	16.37	2.68
10	14448.76	5405.68	7.53	1918.83	457.02	13.23	1.69
11	20189.32	10780.51	8.36	2414.99	820.94	16.65	4.37
12	40713.56	18398.33	7.94	5127.65	1475.16	35.35	5.59

Table 6–Table showing the data generated from the laboratory equipment for UCS and Tensile strength.



## DISCUSSION

Core rock samples of the Travis Peak Formation were collected from Stephen F. Austin State University's core lab repository. Overall 12 samples were collected from different counties based on the depth interval of more than 7500 ft. Samples were restricted to sandstones and any core rocks containing carbonates were avoided. Sandstone samples and carbonate samples like dolomite, limestone, etc., were differentiated by using hydrochloric acid (HCl). If HCl gave a fizz when dropped over the rock samples then it was said to be a carbonate rock; when it did not give any fizz the sample was shown to be a sandstone.

The selected core samples were then cut into a size of 7.2 to 3.6 (in) ratio of length to diameter maintaining the 2 to 1 ratio. Samples were then tested for uniaxial compression test and tensile strength in the Department of Civil Engineering Laboratory at University of Houston. After these tests were performed a regression analysis was used to test the accuracy of the results.

## CONCLUSIONS

In this study a statistical method, regression analysis was carried out to formulate a model that may be used to predict the values of tensile strength given the UCS. Laboratory tests were performed to measure the uniaxial compressive strength and tensile strength of core rock samples of the Travis Peak Formation from certain counties in East Texas.

Uniaxial compressive strength was calculated from the load, which was measured using a compressive test instrument. Load is generated when there is failure at the maximum stress plane ( $\sigma_1$ ). The maximum UCS observed using laboratory tests was 45.87 MPa and the minimum was 13.23 MPa. The average value of UCS for the 12 samples was 27.43 MPa and the standard deviation was 9.47.

Similarly, tensile strength was calculated from the load which was also measured from the same compressive testing instrument. Here, the failure was achieved at the minimum stress plane ( $\sigma_3$ ). The maximum tensile strength observed during the laboratory tests was 6.32 MPa and the minimum was 1.39 MPa. The average value of tensile strength for 12 samples tested was 4.05 MPa and the standard deviation was 1.25.

From Table 5, the rock samples belong to class D, which are medium strength rocks. This can be justified by the mean of the UCS for the rock samples which was 27.43 MPa; Class D classification has a UCS of range 25 – 50 MPa.

Linear regression analysis was performed to build a model so that the values for tensile strength may be predicted given the USC. The R-squared value for the regression analysis was 0.6378, which indicates the model fits fairly well. The slope of the regression equation is 0.1005 which indicates that for each uniaxial compressive strength value the tensile strength is increased by an estimated value of 0.1005.

## FUTURE WORK

This study measured the geotechnical properties of core rocks from the Travis Peak Formation. More geotechnical properties could be measured, like the different types of UCS which includes UCS from Schmidt Hammer and Point load tests depending upon the availability and accessibility to the instruments.

More samples could be collected depending upon the availability and all the necessary factors which were used in this study. More accurate results could be acquired if a larger dataset was used. Some tests that could be done while performing UCS would be specific gravity test, water saturation and dry density.

Soft computing techniques like genetic programming and grey systems will be very useful in comparing the prediction of UCS and tensile strength. Also, different carbonate rocks found in the Travis Peak Formation can also be tested. Then a comparison can be made between the strength of different rock types.

## REFERENCES

- Arkansas Geological Survey. (2016, June 6). *Oil: Petroleum Geology of Producing Area*. Retrieved from [http://www.geology.ar.gov/energy/oil\\_prodarea.htm](http://www.geology.ar.gov/energy/oil_prodarea.htm)
- Arora, M. K., Das Gupta, A. S., & Gupta, R. P. (2004). An artificial neural network approach for landslide hazard zonation in the Bhagirathi (Ganga) Valley, Himalayas. *International Journal of Remote Sensing*, 559-572.
- ASTM D 2938-95. (n.d.). *Standard Test Method for Unconfined Compressive Strength of Intact Rock Core Specimens*.
- ASTM D 3967-95a. (n.d.). *Standard Testing Method for Splitting Tensile Strength of Intact Rock Core Specimens*.
- ASTM D1635. (n.d.). *Standard Test Method for Flexural Strength of Soil-Cement Using Simple Beam with Third-Point Loading*.
- Ayday, C., & Goktan, R. M. (1992). Correlations between L and N type schmidt hammer rebound values obtained during field testing. *Eurock*, (pp. 47-49).
- Baykasoğlu, A., Güllü, H., Çanakçı, H., & Özbakir, L. (2008). Prediction of compressive and tensile strength of limestone via genetic programming. *Expert Systems with Applications*, 111-123.
- Bell, F. G. (2007). Engineering behaviour of sedimentary rocks. In F. G. Bell, *Engineering Geology* (pp. 259-262). Butterworth-Heinemann.
- Bell, F. G., & Culshaw, M. G. (1998). Petrographic and engineering properties of sandstone from the Sneinton Formation, Nottinghamshire, England. *Quarterly Journal Engineering Geology*, 5-21.
- Bieniawski, Z. T. (1984). Rock mechanics design in mining and tunnelling. In Z. T. Bieniawski, *Rock mechanics design in mining and tunnelling* (p. 272). Balkema, Rotterdam.
- Boersma, P., & Weenink, D. (2004, May 11). *Feedforward neural networks 1. What is a feedforward neural network?* Retrieved from Praat: doing phonetics by computer: [http://www.fon.hum.uva.nl/praat/manual/Feedforward\\_neural\\_networks\\_1\\_\\_What\\_is\\_a\\_feedforward\\_ne.html](http://www.fon.hum.uva.nl/praat/manual/Feedforward_neural_networks_1__What_is_a_feedforward_ne.html)
- Broch, E., & Franklin, J. A. (1972). The point load strength test. *International Journal of Rock Mechanics and Mining Sciences*, 669-697.

- Broch, E. (1983). Estimation of Strength Anisotropy Using the Point Load Test. *International Journal of Rock Mechanics and Mining Sciences*, 181-187.
- Brook, N. (1985). The equivalent core diameter method of size and shape correction in point load testing. *International Journal of Rock Mechanics Mining Sciences and Geomechanics*, 61-70.
- Building Research Institute. (2016, June 1). *Material Testing*. Retrieved from Tensile Test on Concrete: <http://www.buildingresearch.com.np/services/mt/mt2.php>
- Bushaw, D. J. (1968). Environmental synthesis of the East Texas Lower Cretaceous: Transactions. *Gulf Coast Association of Geological Societies*, v. XVIII, 416-438.
- Çanakçı, H., Baykasoğlu, A., & Güllü, H. (2009). Prediction of compressive and tensile strength of Gaziantep basalts via neural networks and gene expression programming. *Neural Computing and Applications*, 1031-1041.
- Chambers, J., Cleveland, W., Kleiner, B., & Tukey, P. (1983). *Graphical Methods for Data Analysis*. Wadsworth.
- Collins, E. W., Hobday, D. K., & Kreitler, C. W. (1980). *Quaternary faulting in East Texas*. Austin: University of Texas at Austin, Bureau of Economic Geology Geologic Circular.
- Congalton, R. G. (1991). A review of assessing the accuracy of classifications of remotely sensed data. *Remote Sensing Environment*, 35-46.
- Davidoff, A. J. (1991). Evidence for a deep Mesozoic basin in central east Texas; implications for hydrocarbon exploration. *Gulf Coast Association of Geological Societies*, 143-151.
- Dickinson, K. A. (1969). Upper Jurassic carbonate rocks in northeastern Texas and adjoining parts of Arkansas and Louisiana. *Gulf Coast Association of Geological Societies Transactions*, 175-187.
- Dockery, D. T. (1981). *Stratigraphic column of Mississippi*. Mississippi Bureau of Geology.
- Eaton, R. W. (1956). Resume of subsurface geology of northeast Texas with emphasis on salt structures. *Gulf Coast Association of Geological Societies Transactions*, 79-84.

- ESRI. (2016, May 23). *Regression Analysis Basics*. Retrieved from Regression Analysis Basics:  
[http://resources.esri.com/help/9.3/arcgisdesktop/com/gp\\_toolref/spatial\\_statistics\\_toolbox/regression\\_analysis\\_basics.htm](http://resources.esri.com/help/9.3/arcgisdesktop/com/gp_toolref/spatial_statistics_toolbox/regression_analysis_basics.htm)
- Fener, M., Kahraman, S., Bilgil, A., & Gunaydin, O. (2005). A comparative evaluation of indirect methods to estimate the compressive strength of rocks. *Rock Mech Rock Eng*, 329-343.
- Finley, R. J. (1984). *Geology and engineering characteristics of selected low-permeability gas sandstones: a national survey*. Austin: The University of Texas at Austin, Bureau of Economic Geology, Report of Investigations.
- Foote, R. Q., Massingill, L. M., & Wells, R. H. (1988). *Petroleum geology and the distribution of conventional crude oil, natural gas, and natural gas liquids, East Texas basin*. U.S. Geological Survey Open-File Report.
- Franklin, J. A., & Hoek, E. (1970). Developments in triaxial testing technique. *Rock Mechanics*, 223-280.
- Galloway, W. E. (2009). The Gulf of Mexico Basin has proved to be a highly successful hydrocarbon province, and the vast untapped volume of both oil and gas ensures that the basin will continue as a major player for decades to come. *GeoExPro*.
- Garret, J. H. (1994). Where and why artificial neural networks are applicable in civil engineering. *Journal of Computing in Civil Engineering*, 129-130.
- Geocomp Corp. (2015). *Geocomp Corporation*. Retrieved from Geocomp:  
[http://www.geocomp.com/images/prod\\_images/Unconfined-Compression-mini.jpg](http://www.geocomp.com/images/prod_images/Unconfined-Compression-mini.jpg)
- Gershenson, C. (2003). *Artificial Neural Network for beginners*. Cornell University.
- Ghosh, D. K., & Srivastava, M. (1991). Point load strength: An index for classification of rock material. *Bulletin of International Association of Engineering Geology*, 27-33.
- Hawkins, A. B., & McConnell, B. J. (1992). Sensitivity of sandstone strength and deformability to changes in moisture content. *Quarterly Journal Geological Society*, 115-129.
- Hoek, E., & Brown, E. T. (1980). Empirical strength criterion for rock masses. *Journal of Geotechnical Engineering, ASCE*, 1013-1035.

- Hsu, S. C., & Nelson, P. P. (2002). Characterization of Eagle Ford Shale. *Engineering Geology*, 151-5.
- Indian Standards. (1998). *Method for determination of point load strength index of rocks*. New Delhi: Bureau of Indian Standards.
- ISRM. (1978). Standardization of laboratory and field tests. *International Journal of Rock Mechanics Mining Sciences and Geomechanics*, 319-368.
- ISRM. (1981). *Rock characterization testing and monitoring*. Oxford: Pergamon Press.
- ISRM. (1985). International Society of Rock Mechanics Commission on Testing Methods, Suggested Method for Determining Point Load Strength. *International Journal of Rock Mechanics and Mining Sciences*, 51-60.
- Istone. (n.d.). *Tensile Strength*. Retrieved from Istone:  
[http://www.istone.ntua.gr/Training\\_courses/wp1/3-2-4c-2.jpg](http://www.istone.ntua.gr/Training_courses/wp1/3-2-4c-2.jpg)
- Jackson, M. P. (1982). Fault tectonics of the East Texas Basin. *Bureau of Economic Geology, Geological Circular*, 31.
- Jackson, M. P., & Harris, D. W. (1981). *Sesimic Stratigraphy and salt mobilization along the northwestern margin of the East Texas Basin*, in Kreitler, C. W., and others, *Geology and geohydrology of the East Texas Basin: a report in the progress of nuclear waste isolation feasibility studies*. Austin: The University of Texas at Austin, Bureau of Economic Geology Geological Circular 81-7.
- Jackson, M. P., & Seni, S. J. (1984). *Atlas of salt domes in the East Texas basin*. Bureau of Economic Geology, The University of Texas at Austin.
- Jacobson, L. (2013, December 5). *Introduction to Artificial Neural Networks*. Retrieved from The Project Spot: <http://www.theprojectspot.com/images/post-assets/an.jpg>
- Laerd Statistics. (2016, May 23). *Linear Regression Analysis using SPSS Statistics*. Retrieved from Laerd Statistics: <https://statistics.laerd.com/spss-tutorials/linear-regression-using-spss-statistics.php>
- Lakes, R. (2016, October 9). *What is Poisson's Ratio?* Retrieved from Meaning of Poisson's ratio: <http://silver.neep.wisc.edu/~lakes/PoissonIntro.html>
- Levenberg, K. (1944). A Method for the Solution of Certain Non-linear Problems in Least Squares. *Quarterly of Applied Mathematics*, 164-168.



- Li, Y. (2007, May). Evaluation of Travis Peak Reservoirs, west margin of the East Texas Basin. College Station, Texas, USA.
- Maher Jr., H. D. (2016, May 23). *Geoscience Data Analysis and Modeling*. Retrieved from University of Nebraska Omaha:  
<http://maps.unomaha.edu/maher/GEOL2300/week3/week3.html#anchor438704>
- Marquardt, D. W. (1963). An Algorithm for the Least-Squares Estimation of Nonlinear Parameters. *SIAM Journal of Applied Mathematics*, 431-441.
- Martin, R. G. (1978). Northern and eastern Gulf of Mexico continental margin stratigraphic and structural framework, in Bouma, A. H., Moore, G. T., and Coleman, J. M., eds., Framework, facies, and oil-trapping characteristics of the upper continental margin. *American Association of Petroleum Geologists Studies in Geology*, 21-42.
- Martin, R. G. (1984). *The regional geology, petroleum potential environmental considerations for development, and estimates of undiscovered recoverable oil and gas resources of the United States Gulf of Mexico Continental Margin in the area of proposed Oil and Gas Lease Sales*. U.S. Geological Survey Open-File Report.
- Matlab. (2005). *Neural Network Toolbox*. Retrieved from Conjugate Gradient Algorithms : Backpropagation: <http://matlab.izmiran.ru/help/toolbox/nnet/backpr59.html>
- Mazur, M. (2015, March 17). *A step by step back propagation example*. Retrieved from <https://mattmazur.com/2015/03/17/a-step-by-step-backpropagation-example/>
- McGowen, M. K., & Harris, D. W. (1984). Cotton Valley (Upper Jurassic) and Hosston (Lower Cretaceous) depositional systems and their influence on salt tectonics in the East Texas Basin: in W. P. S. Ventress et al., eds., The Jurassic of the Gulf Rim; Gulf Coast Section SEPM Foundation, *Third Annual Research Conference Proceedings*, (pp. 213-253).
- Meulenkamp, F. (1997). Improving the prediction of the UCS, by equotip readings using statistical and neural network models. *Mem Cent Eng Geol Neth*, 162:127.
- Murray , G. E., & Others. (1985). Introduction to the habitat of petroleum, northern Gulf (of Mexico) coastal province, in Perkins, B. F., and Martin, G. B., Habitat of oil and gas in the Gulf Coast. *Society of Exonomic Paleontologists and Mineralogists Foundation*, (pp. 1-24).
- Newkirk, T. F. (1971). Possible future petroleum potential of Jurassic, western Gulf basin, in Cram, I. H. (ed.), Future petroleum provinces of the United States - their

- geology and potential. *American Association of Petroleum Geologists memoir*, 927-953.
- Nichols, P. H. (1964). The remaining frontiers for exploration in northeast Texas. *Gulf Coast Association of Geological Societies Transactions*, 7-22.
- NIST. (2016). *Engineering Statistics Handbook*. Retrieved from Box Plot: <http://www.itl.nist.gov/div898/handbook/eda/section3/boxplot.htm>
- Palmstrom, A. (2011, March 12). Rmi - A rock mass characterization system for rock engineering purposes. *PhD Thesis*. Oslo, Norway: Oslo University.
- PCTE. (2016, May 31). *PCTE*. Retrieved from The Original Schmidt Hammer: <http://pcte.com.au/images/NDT-Equipment-images/SchmidtHammer/2.jpg>
- Presco. (2013). *Presco Inc.*. Retrieved from <http://www.prescocorp.com/projects/east%20texas/stratcolumn.gif>
- Proceq. (2016, May 31). *Proceq*. Retrieved from Proceq USA E Shop: [http://shop-usa.proceq.com/product\\_info.php?cPath=0\\_23\\_91\\_97&products\\_id=167&osCsid=i9jqk0bcv3g2m4ugotdb2to7g5](http://shop-usa.proceq.com/product_info.php?cPath=0_23_91_97&products_id=167&osCsid=i9jqk0bcv3g2m4ugotdb2to7g5)
- Rainwater, E. H. (1960). Straigraphy and its role in future exploration of oil and gas in Gulf Coast. *Gulf Coast Association of Geological Societies Transactions*, 33-75.
- Rainwater, E. H. (1968). Geological history of oil and gas potential of the Central Gulf Coast. *Gulf Coast Association of Geological Societies Transactions*, 124-165.
- Rainwater, E. H. (1970). Regional Stratigraphy and petroleum potential of Gulf Coast Lower Cretaceous. *Gulf Coast Association of Geological Societies Transactions*, 145-157.
- Ramamurthy, T., & Arora, V. K. (1993). A classification for intact and jointed rocks. *Geotechnical engineering of hard soils-soft rocks*, 235-242.
- Rao, K. S., Rao, G. V., & Ramamurthy, T. (1987). Strength of sandstones in saturated and partially saturated conditions. *Geotechnical Engineering*, 99-127.
- Salvador, A. (1987). Late Triassic-Jurassic paleogeography and origin of Gulf of Mexico Basin. *AAPG Bulletin*, 419-451.
- Saucier, A. E. (1985). *Geologic Framework of Travis Peak (Hosston) Formation of East Texas and Louisiana, in Finley, R. J., et al., The Travis peak Formation: Geologic Framework, core studies and engineering field analysis*. The University of Texas at Austin, Bureau of Economic Geology, contract report n0. GRI-85/0044 prepared for the Gas Research Institute under contract no. 5082-211-0708.

- Schalkoff, R. J. (1997). *Artificial Neural Networks*. McGraw-Hill.
- Seibi, A., & Al-Alawi, S. M. (1997). Prediction of fracture toughness using artificial neural networks. *Engineering Fracture Mechanics*, 311-319.
- Singh, V. K., Singh, D., & Singh, T. N. (2001). Prediction of strength properties of some schistose rocks from petrographic properties using artificial neural networks. *International Journal of Rock Mechanics and Mining Sciences*, 269-284.
- Statistics Solutions. (2013). *What is Linear Regression*. Retrieved from Statistics Solutions: <http://www.statisticssolutions.com/what-is-linear-regression/>
- Tye, R. S. (1989). Fluvial sandstone reservoirs of Travis Peak (Hosston) Formation, East Texas Basin. *AAPG Bulletin*, v. 73, 421.
- University of Washington. (2016, May 23). *Linear Regression*. Retrieved from ATM S 451 Lab Manual: <http://www.atmos.washington.edu/~robwood/teaching/451/labs/linearregression.html>
- Vail, P. R., & et al. (1977). Seismic stratigraphy and global changes of sea level. *Seismic stratigraphy - applications to hydrocarbon exploration* (pp. 49-212). American Association of Petroleum Geologists.
- Warner, J. A. (1993). *Regional geologic framework of the Cretaceous, offshore Mississippi*. Jackson: Mississippi Department of Environmental Quality.
- Wood, D. H., & Guevara, E. H. (1981). *Regional structural cross sections and general stratigraphy, East Texas Basin*. Austin: The University of Texas at Austin, Bureau of Economic Geology Cross Sections.
- Yates, P. G. (1992). The material strength of sandstones of the Sherwood Sandstone Group of north Staffordshire with reference to microfabirc. *Quarterly Journal Geological Society*, 107-113.

**APPENDIX A – CORE SAMPLES DATABASE**

Table 7 - Table showing details on the core samples that must be used for the testing.

<b>API</b>	<b>NumberOfBoxes</b>	<b>X</b>	<b>Y</b>	<b>Depth</b>	<b>County</b>
<b>03730288</b>	17	-94.0674141	33.3180697	9000	Bowie
<b>06730432</b>	2			6100	Bowie
<b>06730434</b>	2	-94.1361712	32.9964246	6100	Bowie
<b>06730469</b>	2	-94.1328450	33.0016427	6100	Bowie
<b>06730472</b>	1	-94.1428303	32.9881211	6093	Bowie
<b>06730475</b>	2	-94.1203544	33.0064686	6100	Bowie
<b>06730477</b>	2	-94.1237491	33.0065534	6100	Bowie
<b>06730478</b>	2	-94.1183602	33.0093725	6100	Bowie
<b>06730482</b>	2				
<b>06730484</b>	2	-94.1217662	33.0089595	6100	Bowie
<b>06730488</b>	2	-94.1143441	33.0099487	6100	Bowie
<b>06730489</b>	2	-94.1412647	32.9854973	6100	Bowie
<b>06730547</b>	20	-94.1140637	33.0077657	6100	Bowie
<b>06730577</b>	2	-94.1381949	32.9770992	6100	Bowie
<b>06730714</b>	18	-94.0674045	33.0241065	6100	Bowie
<b>10539584</b>	126	-101.9040465	30.9620919	6100	Bowie
<b>10539639</b>	131	-101.8844747	30.9692479	6100	Bowie
<b>10539658</b>	4	-101.8992749	30.9725194	6100	Bowie
<b>10539819</b>	2	-101.8683593	30.9835001	6100	Bowie
<b>10539885</b>	2	-101.8520433	30.8987167	6100	Bowie
<b>10539889</b>	65	-101.8781112	30.9805555	6100	Bowie
<b>10539910</b>	50	-101.8030972	30.9415267	6100	Bowie
<b>10540041</b>	2	-101.8986619	30.9945668	6100	Bowie
<b>10540055</b>	27	-101.8454651	30.919604	6100	Bowie
<b>10540290</b>	101	-101.830308	30.886847	6100	Bowie
<b>10540334</b>	18	-101.833909	30.887273	6100	Bowie
<b>10540345</b>	1	-101.8383039	30.882586	6100	Bowie
<b>16131229</b>	25	-96.3418012	31.7362474	12000	Freestone
<b>16131409</b>	5	-96.2223344	31.6203672	12000	Freestone
<b>18330958</b>	8	-94.8319258	32.5383259	7500	Freestone
<b>18331297</b>	21	-94.9334652	32.5505917	10000	Gregg

<b>20332171</b>	<b>3</b>	<b>-94.0785006</b>	<b>32.5097246</b>	<b>5900</b>	<b>Gregg</b>
<b>20332249</b>	<b>15</b>	<b>-94.1103075</b>	<b>32.4230525</b>	<b>2700</b>	<b>Gregg</b>
<b>20332253</b>	<b>5</b>	<b>-94.0679832</b>	<b>32.469908</b>	<b>2700</b>	<b>Gregg</b>
<b>20332348</b>	<b>9</b>	<b>-94.649061</b>	<b>32.7018649</b>	<b>3700</b>	<b>Gregg</b>
<b>20332350</b>	<b>1</b>	<b>-94.6870034</b>	<b>32.7093313</b>	<b>3800</b>	<b>Gregg</b>
<b>20332415</b>	<b>20</b>	<b>-94.6337798</b>	<b>32.7034887</b>	<b>3600</b>	<b>Gregg</b>
<b>20332558</b>	<b>5</b>	<b>-94.392921</b>	<b>32.4646912</b>	<b>6000</b>	<b>Gregg</b>
<b>21330756</b>	<b>35</b>	<b>-95.571681</b>	<b>32.0686618</b>	<b>9900</b>	<b>Gregg</b>
<b>21330787</b>	<b>6</b>	<b>-95.93317</b>	<b>32.0932446</b>	<b>8400</b>	<b>Henderson</b>
<b>26932697</b>	<b>1</b>	<b>-100.0611654</b>	<b>33.6986735</b>	<b>8400</b>	<b>Henderson</b>
<b>27730116</b>	<b>6</b>	<b>-95.4043176</b>	<b>33.5384112</b>	<b>8400</b>	<b>Henderson</b>
<b>31530855</b>	<b>4</b>	<b>-94.2468561</b>	<b>32.7741368</b>	<b>8400</b>	<b>Henderson</b>
<b>31530874</b>	<b>2</b>	<b>-94.2498675</b>	<b>32.7770898</b>	<b>8400</b>	<b>Henderson</b>
<b>36501107</b>	<b>4</b>	<b>-94.1186202</b>	<b>32.1811946</b>	<b>3080</b>	<b>Henderson</b>
<b>36530251</b>	<b>13</b>	<b>-94.2259916</b>	<b>32.0975177</b>	<b>2050</b>	<b>Henderson</b>
<b>36533070</b>	<b>52</b>	<b>-94.0855906</b>	<b>32.3779916</b>	<b>4900;6000</b>	<b>Henderson</b>
<b>36533106</b>	<b>14</b>	<b>-94.0849156</b>	<b>32.3814072</b>	<b>6000</b>	<b>Henderson</b>
<b>36534070</b>	<b>20</b>	<b>-94.2701039</b>	<b>32.2419251</b>	<b>2000</b>	<b>Henderson</b>
<b>36534131</b>	<b>7</b>	<b>-94.2580663</b>	<b>32.2433188</b>	<b>1900</b>	<b>Henderson</b>
<b>36534339</b>	<b>17</b>	<b>-94.2329432</b>	<b>32.1307754</b>	<b>2400</b>	<b>Henderson</b>
<b>36534412</b>	<b>14</b>	<b>-94.2086483</b>	<b>32.1192522</b>	<b>2020</b>	<b>Henderson</b>
<b>36534662</b>	<b>4</b>	<b>-94.2511633</b>	<b>32.0799161</b>	<b>2000</b>	<b>Henderson</b>
<b>36534663</b>	<b>5</b>	<b>-94.2618742</b>	<b>32.1016286</b>	<b>2080</b>	<b>Henderson</b>
<b>36534711</b>	<b>19</b>	<b>-94.2375459</b>	<b>32.113753</b>	<b>2030</b>	<b>Henderson</b>
<b>37137724</b>	<b>38</b>	<b>-101.9034488</b>	<b>30.7767471</b>	<b>2030</b>	<b>Henderson</b>
<b>37137890</b>	<b>3</b>	<b>-102.0375083</b>	<b>30.7419903</b>	<b>2030</b>	<b>Henderson</b>
<b>37137893</b>	<b>1</b>	<b>-102.2420308</b>	<b>30.7931677</b>	<b>2030</b>	<b>Henderson</b>
<b>37137965</b>	<b>1</b>	<b>-102.3228716</b>	<b>30.8219172</b>	<b>2030</b>	<b>Henderson</b>
<b>37137966</b>	<b>1</b>	<b>-102.3248371</b>	<b>30.8049302</b>	<b>2030</b>	<b>Henderson</b>
<b>37137986</b>	<b>1</b>	<b>-102.2380443</b>	<b>30.7377889</b>	<b>2030</b>	<b>Henderson</b>
<b>37138075</b>	<b>2</b>	<b>-102.0373358</b>	<b>30.7417314</b>	<b>2030</b>	<b>Henderson</b>
<b>37138376</b>	<b>1</b>	<b>-102.2475118</b>	<b>30.7971403</b>	<b>2030</b>	<b>Henderson</b>
<b>37330782</b>	<b>20</b>	<b>-94.8242608</b>	<b>30.7681475</b>	<b>2030</b>	<b>Henderson</b>
<b>37930137</b>	<b>18</b>	<b>-95.7954869</b>	<b>32.8253506</b>	<b>13000</b>	<b>Henderson</b>
<b>37930149</b>	<b>3</b>	<b>-95.7670569</b>	<b>32.798112</b>	<b>13000</b>	<b>Rains</b>
<b>38730464</b>	<b>5</b>	<b>-95.165652</b>	<b>33.5224484</b>	<b>13000</b>	<b>Rains</b>

<b>38730486</b>	<b>1</b>	-94.8213889	33.5511111	<b>13000</b>	<b>Rains</b>
<b>38730497</b>	<b>1</b>	-95.2439157	33.5022272	<b>13000</b>	<b>Rains</b>
<b>38730523</b>	<b>2</b>	-95.133897	33.5351932	<b>13000</b>	<b>Rains</b>
<b>38730535</b>	<b>2</b>	-95.0775534	33.5620329	13000	<b>Rains</b>
<b>39934530</b>	<b>14</b>	-100.0964299	31.8854934	13000	<b>Rains</b>
<b>39934585</b>	<b>16</b>	-100.0944979	31.8981763	13000	<b>Rains</b>
<b>39934606</b>	<b>20</b>	-100.092041	31.8958954	13000	<b>Rains</b>
<b>39934624</b>	<b>61</b>	-100.0959896	31.8824011	13000	<b>Rains</b>
<b>39934666</b>	<b>8</b>	-100.095106	31.8779573	13000	<b>Rains</b>
<b>40132413</b>	<b>10</b>	-94.9174135	32.2035035	<b>3500</b>	<b>Rains</b>
<b>42331387</b>	<b>3</b>	-94.990705	32.2314682	<b>7200</b>	<b>Smith</b>
<b>42331406</b>	<b>6</b>	-95.0515868	32.314011	<b>7700</b>	<b>Smith</b>
<b>42331415</b>	<b>16</b>	<b>-95.2253550</b>	32.2717298	<b>4600</b>	<b>Smith</b>
<b>42331446</b>	<b>3</b>	-95.22781	32.3439561	<b>7200</b>	<b>Smith</b>
<b>42331510</b>	<b>9</b>	-95.4255691	32.3603624	<b>7800</b>	<b>Smith</b>
<b>42331645</b>	<b>12</b>	-95.1523346	32.2036099	<b>8400</b>	<b>Smith</b>
<b>45930714</b>	<b>8</b>	-95.0174568	32.6353425	<b>840</b>	<b>Smith</b>
			<b>0</b>		
<b>46730817</b>	<b>14</b>	-95.878955	32.3987724	8400	<b>Smith</b>
<b>46730877</b>	<b>1</b>	-95.878955	32.3987724	<b>8700</b>	<b>Van Zandt</b>
<b>46730897</b>	<b>21</b>	-95.9216432	32.4586407	<b>8200</b>	<b>Van Zandt</b>
<b>49931800</b>	<b>2</b>	-95.380293	32.7095197	<b>9500</b>	<b>Van Zandt</b>
<b>49931819</b>	<b>27</b>	-95.6386104	32.9026841	<b>13000</b>	<b>Van Zandt</b>
<b>49931982</b>	<b>7</b>	-95.3848936	32.6846467	<b>8900</b>	<b>Wood</b>

## APPENDIX B – HAND SAMPLE DESCRIPTIONS



Color – Gray

Predominant Mineral Composition – Quartz, Feldspar and Rock fragments

Particle size – Very fine

No Laminations

Fractures – Unfractured





Color – Gray

Predominant Mineral Composition – Quartz, Feldspar and Rock fragments

Particle size – Very fine

Thin laminations

Fractures – Unfractured

Hardness – Moderately Hard rock





Color – Gray

Predominant Mineral Composition – Quartz, Feldspar and Rock fragments

Particle size – Very fine

No laminations

Fractures – Unfractured

Hardness – Moderately Hard rock



Color – Gray

Predominant Mineral Composition – Quartz, Feldspar and Rock fragments

Particle size – Very fine

No laminations

Fractures – Unfractured

Hardness – Moderately Hard rock





Color – Gray

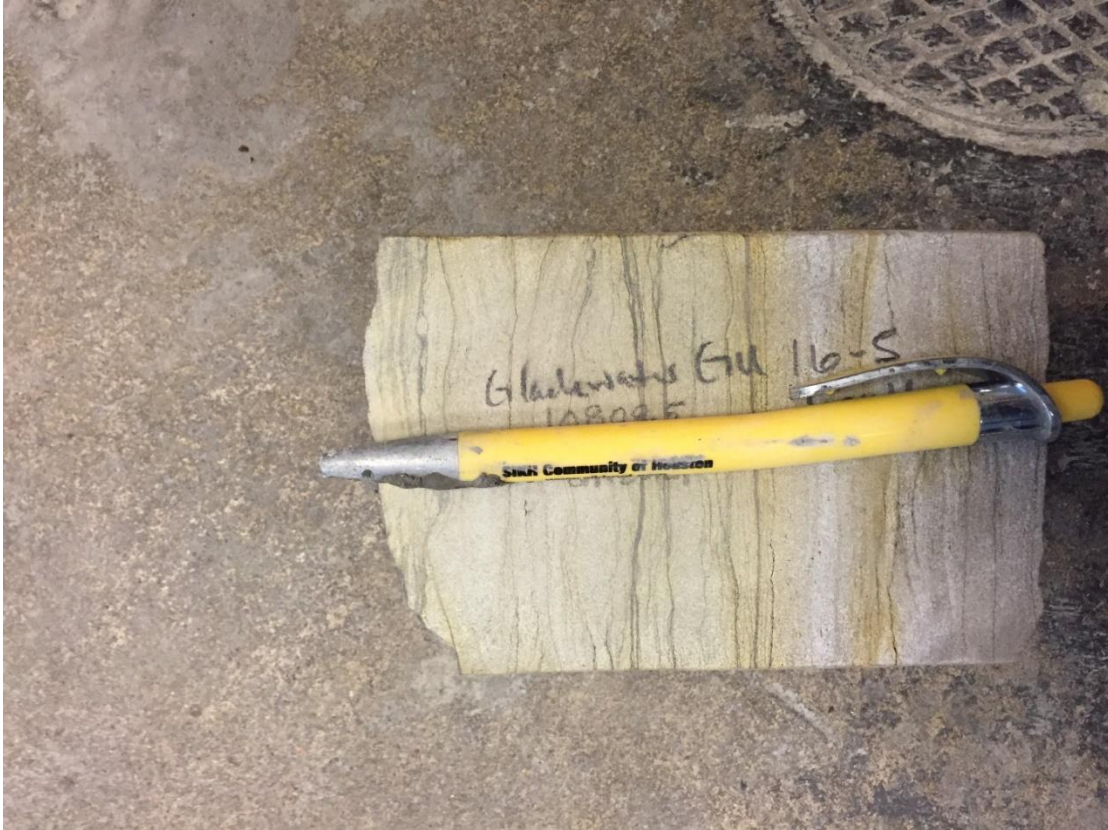
Predominant Mineral Composition – Quartz, Feldspar and Rock fragments

Particle size – Very fine

No laminations

Fractures – Unfractured

Hardness – Moderately Hard rock



Color – Light yellow

Predominant Mineral Composition – Quartz, Feldspar and Rock fragments

Particle size – Very fine

Thinly laminated

Fractures – Unfractured

Hardness – Moderately Hard rock



Color – Gray

Predominant Mineral Composition – Quartz, Feldspar and Rock fragments

Particle size – Very fine

No laminations

Fractures – Unfractured

Hardness – Moderately Hard rock





Color – Gray

Predominant Mineral Composition – Quartz, Feldspar and Rock fragments

Particle size – Very fine

No laminations

Fractures – Unfractured

Hardness – Moderately Hard rock



Color – Gray

Predominant Mineral Composition – Quartz, Feldspar and Rock fragments

Particle size – Very fine

No laminations

Fractures – Unfractured

Hardness – Moderately Hard rock

## VITA

Pawan Kakarla graduated from Narayana Junior College in Vijayawada, Andhra Pradesh, India, in May of 2008. Pawan attended Indian Institute of Technology, Roorkee, India from the Fall of 2008 to the Spring of 2013, where he graduated with an Integrated M. Tech in Geological Technology. After receiving his master's degree, Pawan began working on his M.S. in Geology at Stephen F. Austin State University in August of 2014 where he graduated in August of 2016.

Permanent Address:

118, Sitapuram Colony, Poranki

Vijayawada, Andhra Pradesh, 521137,

India

Style: Geological Society of America

This thesis was typed by Pawan Kakarla